Assessing the power law distribution of TGFs

Andrew B. Collier,[1,2,3] Thomas Gjesteland,[3] and Nikolai Østgaard[3]

[1]   The times and locations of 972 TGFs detected by Reuven Ramaty High Energy Solar Spectroscopic Imager (RHESSI) between 4 March 2002 and 6 September 2010 were compared to lightning data for the same period. Based on a simple coincidence algorithm, 93 TGFs were uniquely matched to individual lightning discharges. The average delay between the lightning and the associated TGF was −0.77 ms, suggesting that the TGFs occurred prior to the lightning discharge. The majority of the matched lightning occurred within 500 km of the RHESSI sub-satellite point, although a few events were found at larger distances. A comparison of TGF intensity to observation angle for the matched events was found to be consistent with a power law model for the distribution of TGF intensities. Finally it was found that the matched TGFs were predominantly those of lower intensity.

Citation: Collier, A. B., T. Gjesteland, and N. Østgaard (2011), Assessing the power law distribution of TGFs, *J. Geophys. Res.*, *116*, A10320, doi:10.1029/2011JA016612.

1. Introduction

1.1. Overview

[2]   A Terrestrial Gamma-ray Flash (TGF) is a brief ($\lesssim 1$ ms) pulse of γ-rays with energies extending up to around 40 MeV, and average energy ~2 MeV [*Smith et al.*, 2005; *Briggs et al.*, 2010; *Marisaldi et al.*, 2010]. TGFs are detected by satellites in Low Earth Orbit (LEO) and have been identified by the Burst and Transient Source Experiment (BATSE) on the Compton Gamma-Ray Observatory (CGRO) [*Fishman et al.*, 1994], RHESSI [*Smith et al.*, 2005], Astrorivelatore Gamma a Immagini Leggero (AGILE) [*Marisaldi et al.*, 2010] and Fermi Gamma-ray Burst Monitor (GBM) [*Briggs et al.*, 2010].

[3]   TGFs exhibit both spatial and temporal correlations with lightning activity [*Fishman et al.*, 1994; *Inan et al.*, 1996; *Smith et al.*, 2005; *Marisaldi et al.*, 2010; *Briggs et al.*, 2010]. Although this relationship was initially qualitative, a number of TGFs have subsequently been linked to specific storms [*Smith et al.*, 2010], individual sferics [*Inan et al.*, 1996, 2006; *Cummer et al.*, 2005; *Stanley et al.*, 2006; *Cohen et al.*, 2006] or specific lightning discharges [*Cohen et al.*, 2010; *Connaughton et al.*, 2010a].

1.2. Mechanism

[4]   TGFs are thought to be generated by bremsstrahlung emissions from a deluge of energetic electrons. *Wilson* [1925] made the prescient suggestion that electrons could gain energy through acceleration by an electric field either within or above a thundercloud, and subsequently lose energy via radiative collisions with atmospheric nuclei. These ideas were later expanded to the generation of a Relativistic Runaway Electron Avalanche (RREA), where the electrostatic force on relativistic electrons exceeds atmospheric drag, leading to sustained acceleration, and secondary ionization rapidly inflates the profusion of energetic particles [*Gurevich et al.*, 1992; *Roussel-Dupré et al.*, 1998; *Gurevich and Milikh*, 1999; *Lehtinen et al.*, 1999; *Dwyer*, 2003, 2007]. The electric field required for RREA is appreciably smaller than that for conventional dielectric breakdown. While the high energy tail of the resulting electron distribution is responsible for the generation of γ-rays, the aggressive population growth is driven by 3–200 keV electrons [*Milikh and Roussel-Dupré*, 2010].

[5]   The source of the accelerating electric field remains a topic of speculation, with possible candidates including the ambient electric field resulting from charge separation within a thundercloud, the quasistatic remnant field after a lightning discharge or the potent but ephemeral fields in lightning streamers and leaders. TGFs were initially thought to be related to red sprites [*Nemiroff et al.*, 1997], motivating the proposal of a mechanism based on quasistatic electric fields [*Lehtinen et al.*, 1996]. However, quasistatic fields were found to only be effective at altitudes less than 20 km [*Lehtinen et al.*, 1999], inconsistent with TGF production altitudes which were thought to be higher at that time. This led to the suggestion of a mechanism based on electromagnetic pulses [*Milikh and Valdivia*, 1999; *Inan and Lehtinen*, 2005]. The scarcity of lightning discharges able to activate either of these mechanisms contradicts the observed frequency of TGFs. Alternative theories propose the repulsive force of the mobile negative tip of lightning leaders and streamers, present at lower altitudes within thunderclouds [*Moss et al.*, 2006; *Dwyer*, 2008; *Carlson et al.*, 2009, 2010]. These ideas are supported by observations of X-rays associated with stepped leaders [*Moore et al.*,

---

[1]SANSA Space Science, Hermanus, South Africa.
[2]School of Physics, University of KwaZulu-Natal, Durban, South Africa.
[3]Department of Physics and Technology, University of Bergen, Bergen, Norway.
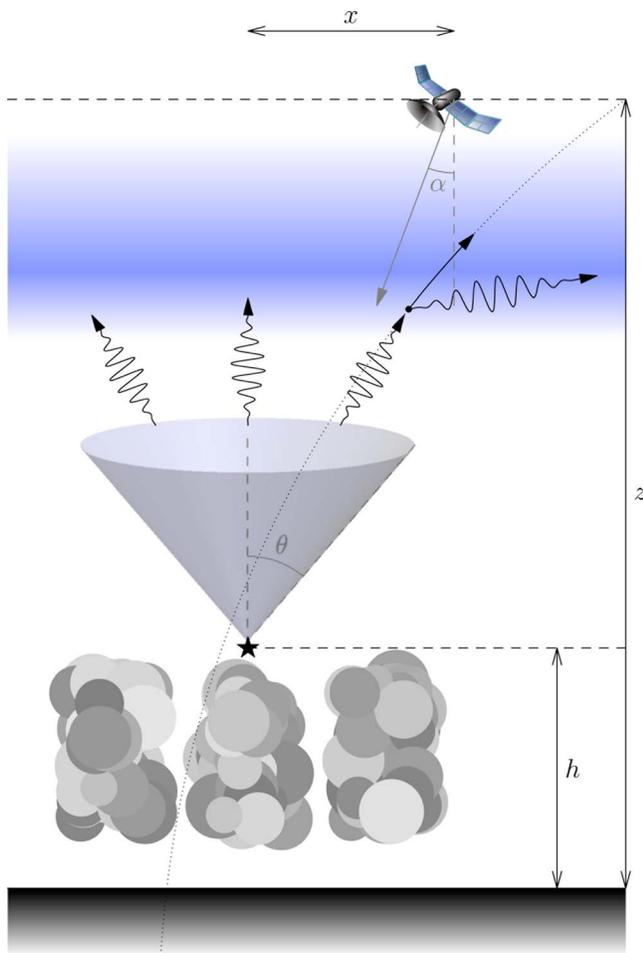
Figure 1. Schematic illustration of the observation of a TGF by a LEO satellite (not to scale). The photons are emitted at altitude h into a source cone of half-width θ. The satellite is located at altitude z with sub-satellite point a distance x from the TGF source. The angle at the satellite between the nadir direction and the TGF source is α.

2001; *Dwyer et al.*, 2005], where the X-ray source is coincident and collocated with leader step electric field changes [*Howard et al.*, 2008]. Each of these hypotheses has consequences for the temporal relationship between the TGF and the lightning discharge. For the quasistatic field and electromagnetic pulse mechanisms the TGF would necessarily follow after the lightning. The lightning current pulse in leaders and streamers or the ambient electric field would yield a TGF coincident with or preceding the lightning.

[6] A seed population of relativistic electrons is also required to induce a RREA. One possible source is cosmic rays, although these alone are probably inadequate [*Carlson et al.*, 2008; *Dwyer*, 2008]. Alternatively, thermal electrons can be accelerated to the required energies by the acute electric fields in streamer tips [*Moss et al.*, 2006]. *Dwyer* [2007] proposed a feedback mechanism which can regenerate seed electrons from back-scattered energetic photons and positrons, leading to a RREA able to rapidly discharge an intense localized electric field. The dissolution of this localized electric field does not necessarily preclude the initiation of lightning elsewhere in the thundercloud. However, if a TGF were generated by the RREA itself then this also leaves open the possibility of a TGF without an accompanying lightning discharge.

[7] The total energy radiated by a TGF is ~1 kJ [*Briggs et al.*, 2010], although this may vary substantially depending on the parameters of the emission process [*Carlson et al.*, 2007, Figure 3]. A simple bremsstrahlung model indicates that the source electrons must have energies in the range 20–40 MeV, although the upper limit can only be accurately determined from the high energy cutoff in the observed photon spectra [*Smith et al.*, 2005].

1.2.1. Electron Events

[8] The primary runaway electrons are ultimately lost to collisions with the atmosphere before reaching LEO. In the rarefied upper atmosphere above ~40 km, secondary electrons and positrons are able to escape and stream out into the inner magnetosphere along the Earth's magnetic field lines [*Lehtinen et al.*, 2001; *Dwyer et al.*, 2008]. The relatively narrow electron-positron beam may be detected at LEO on these magnetic field lines either in the vicinity of the TGF or near the conjugate point [*Dwyer et al.*, 2008; *Briggs et al.*, 2011]. The likelihood of a satellite intercepting such a beam is considerably smaller than that of exposure to the relatively broad cone of γ-rays. Despite this, such events have indeed been observed [*Briggs et al.*, 2010; *Connaughton et al.*, 2010a], with one particularly compelling candidate observed by RHESSI over the Sahara [*Smith et al.*, 2006]. Another fainter event was observed by RHESSI over the Middle East, although the statistical significance of this event was marginal [*Smith et al.*, 2006]. In both cases thunderstorm activity was located close to the conjugate point.

1.3. Schematic Illustration

[9] A schematic illustration of the accepted TGF generation scenario is given in Figure 1. The γ-ray photons are emitted at altitude h into a cone of half-angle θ. Some fraction of these photons is observed by a LEO satellite at altitude z displaced horizontally from the TGF by distance x. The small influence of the Earth's curvature must be taken into account when determining x and the observation angle, α, between the satellite nadir and the TGF source.

[10] Although the TGF emission source is illustrated as a point, the radiation process must occur within some finite volume. *Briggs et al.* [2010] placed an upper bound ~50 km on the emission region radius. However, based on a typical time scale of 50 μs the source region might be smaller than ~15 km [*Nemiroff et al.*, 1997; *Dwyer*, 2008].

1.3.1. Source Altitude

[11] The source altitude has a profound effect on the time evolution, intensity and spectrum of TGF photons, and must be a compromise between two extremes: high altitude sources lack sufficient atmosphere to produce the required radiation, while low altitude sources are onerously attenuated.

[12] The intrinsic bremsstrahlung radiation spectrum scales inversely with photon energy and is thus dominated by less energetic photons. An observed TGF spectrum is not, however, a direct reflection of the source distribution but is affected by the depth of atmosphere through which the radiation travels, and is thus very sensitive to the production altitude and observation angle. Low energy photons are

most susceptible to atmospheric absorption, causing a flattening of the spectrum. TGFs produced at higher altitudes thus have a softer spectrum and a reduced low-energy cutoff [*Østgaard et al.*, 2008]. The spectra also exhibit a high-energy cutoff which declines with increasing α [*Østgaard et al.*, 2008]. This cutoff places an upper limit on the Compton scattering angles [*Gjesteland et al.*, 2011], which in turn constrains the width of the source beam.

[13] *Williams et al.* [2006] provide a simple analytical demonstration for the strong dependence of γ-ray flux on source altitude. Since the upper atmosphere is essentially transparent to γ-rays, photons generated at high altitudes are quite likely to reach LEO. The mean free path for γ-rays at low altitudes is shorter than the atmospheric scale height so that they are rapidly attenuated, leading to the initial assumption of a high TGF production altitude. A source located in the upper troposphere or lower stratosphere (15–21 km) is thus more likely to be detected than one lower in the troposphere (~5 km) [*Williams et al.*, 2006]. Despite the severe attenuation, the vast number of γ-rays generated by a TGF result in some residual photons reaching LEO. A small increase in source altitude can thus result in a massive increase in the observed flux.

[14] Although originally thought to originate at high altitudes in association with intense Cloud-to-Ground (CG) lightning, recent spectral analyses and correlations with lightning data suggest that TGFs are produced at lower altitudes. The averaged spectra from BATSE and RHESSI TGFs consistently indicated that $h \sim 15$–20 km [*Dwyer and Smith*, 2005; *Carlson et al.*, 2007]. Analysis of individual BATSE spectra revealed two possible source ranges, $h \leq 20$ km and $h \sim 30$–40 km [*Østgaard et al.*, 2008]. However, *Gjesteland et al.* [2010] subsequently illustrated that the latter range was biased by instrumental deadtime and presented revised results with lower h. *Cummer et al.* [2005] found that the paltry lightning charge moment changes associated with TGFs confine the production altitude to $h < 30$ km. *Stanley et al.* [2006] and *Shao et al.* [2010] found that $h \sim 10$–15 km. All of these observations are broadly compatible with a production altitude of $h \lesssim 20$ km. Complete attenuation of radiation from events at low altitudes leads to an altitude floor in observations. However, a minimum TGF production altitude does not arise from considerations of the generation mechanism.

1.3.2. Beam Width

[15] The particulars of the source beam are determined by the motion of the relativistic electrons. The collimated motion of the electrons and the forward directed peak in the bremsstrahlung cross section should lead to an anisotropic emission [*Inan and Lehtinen*, 2005]. Acceleration in a large scale electric field will generate a narrow emission beam, while photons resulting from current pulses in lightning leaders would have a broad directional distribution [*Carlson et al.*, 2009].

[16] The model source cone can extend from a narrow beam (small θ) to half-isotropic ($\theta \sim 90°$). A realistic beam width is still a matter of some uncertainty. *Østgaard et al.* [2008] concluded that θ must be relatively small to account for the many soft TGF spectra observed. Yet the observations of TGFs at large α suggest that θ is still reasonably large. *Hazelton et al.* [2009] demonstrated that a

narrow beam at $h \geq 21$ km was inconsistent with observations at $x > 300$ km, espousing instead a wide emission beam originating at $h \sim 15$ km. *Carlson et al.* [2007] and *Dwyer and Smith* [2005] found that $\theta \sim 45°$ gave a good fit to RHESSI data. *Gjesteland et al.* [2011] conclude that $30° \leq \theta \leq 40°$, suggesting a weakly divergent electric field consistent with the ambient field within a thundercloud.

1.3.3. Observation Angle

[17] Photons lose energy to electron kinetic energy via Compton scattering, where the energy decrement is determined by the scattering angle. Compton scattering thus degrades the population of source photons by reducing the intensity, softening the spectrum and broadening the beam [*Østgaard et al.*, 2008; *Hazelton et al.*, 2009]. While the low energy component of the observed spectrum consists of photons which have lost energy in numerous scattering interactions, high energy photons are likely to have travelled unimpeded [*Gjesteland et al.*, 2010]. There exists a profound difference in the spectra and temporal evolution of the photons in direct ($\alpha \leq \theta$) and scattered ($\alpha > \theta$) events [*Østgaard et al.*, 2008]. Whereas for $\alpha \leq \theta$ the observed spectrum will consist both of photons which have propagated uninterrupted from the source and photons which have scattered en route, for $\alpha > \theta$ only scattered photons are observed. Within the direct beam, TGF spectra become progressively harder with increasing α due to the fact that high energy photons are unimpeded, while lower energy photons undergo multiple Compton scattering interactions, reducing their energy and broadening their angular distribution. Outside the direct beam all photons have been scattered so that the fluence is reduced and the spectra are thus softer and possess a high energy cutoff. The photons also incur a time delay due to the longer path travelled [*Østgaard et al.*, 2008; *Grefenstette et al.*, 2008].

[18] In principle the likelihood of observing scattered events is higher since the ionospheric projection of the direct beam is smaller than that of the diffuse, scattered beam. However, the intensity of scattered events is significantly lower, so that the majority fall beneath the detection threshold. The sensitivity of the instrument thus determines how many of the diffuse events are identified. The impact of the detection threshold is reduced for larger θ since more of events are then direct.

1.4. Characteristics of Causative Lightning

[19] The characteristics of a TGF are completely determined by the properties of the accelerating electric field which, in turn, is intimately connected to the details of the causative lightning discharge. TGFs are associated with tall tropical thunderstorms with cloud top heights between 13.6 and 17.3 km [*Splitt et al.*, 2010]. Although thunderstorm anvils do occasionally penetrate to higher altitudes, they are generally confined below the tropopause which is located at around 20 km altitude at the equator and descends at higher latitudes.

[20] The mean charge moment change associated with TGF producing lightning strokes was found to be 49 C km [*Cummer et al.*, 2005], which is relatively meagre compared to typical sprite producing lightning, and considerably too small for the quasistatic electric field mechanism [*Lehtinen et al.*, 2001]. A charge moment in this range is characteristic

of Intra-Cloud (IC) lightning [*Williams et al.*, 2006]. *Cummer et al.* [2005] suggested that TGFs may be produced prior to a lightning discharge of modest intensity, where the TGF mechanism is connected to the development of the lightning discharge rather than the discharge itself.

1.4.1. Case Against CG

[21] *Inan et al.* [2006] found that a large proportion of TGFs were associated in time and azimuth with sferics detected at Palmer Station, Antarctica. The intensity of these sferics indicated that they were generated by particularly powerful lightning discharges. But *Williams et al.* [2006] observed that the causative lightning strokes associated with TGFs were not the vigorous +CG discharges resulting in Transient Luminous Events (TLE), since these occur at low altitude and any γ-rays produced would be attenuated before achieving LEO. Furthermore, the charge moments associated with TGFs are far smaller than those required to initiate TLEs [*Cummer et al.*, 2005]. Although TLEs only occur above large thunderstorm systems [*Sentman and Wescott*, 1995], TGFs are generated by thunderstorms with a wide range of magnitudes [*Splitt et al.*, 2010]. Finally, the tight coupling of TGFs to the causative lightning strokes is completely dissimilar to the time scales of sprites, which lag $\Delta t \sim$ 5–10 ms behind the causative lightning discharge [*Lyons*, 1996; *Li et al.*, 2008].

1.4.2. Case in Favor of IC

[22] IC lightning, between charge centers in one or more clouds, is far more common than CG lightning [*Mackerras et al.*, 1998], especially close to the equator [*Mushtak et al.*, 2005]. High altitude IC lightning can occur up to ~15 km, particularly at low latitudes where the tropopause is high [*Williams et al.*, 2006].

[23] *Williams et al.* [2006] systematically eliminated all varieties of lightning discharge except IC as viable candidates for a TGF source and found that Extremely Low Frequency (ELF) measurements of positive polarity lightning coincident with RHESSI events were compatible with ascending negative leaders. *Stanley et al.* [2006] found that lightning associated with TGFs was consistent with intense (upper 5%) positive polarity IC discharges transporting electrons upward. Recently, *Shao et al.* [2010] discerned a link between RHESSI TGFs and IC lightning transporting negative charge upward, with typical peak currents <10 kA. *Lu et al.* [2010] found a peak current of 36 kA for a single TGF originating during the development of a compact IC discharge between charge centers at 8.5 and 13 km altitude.

[24] TGFs generally occur during the declining phase of thunderstorm activity [*Smith et al.*, 2010], which is a disconcerting result given that the period of most abundant IC lightning precedes that for CG lightning [*Williams et al.*, 1989]. *Smith et al.* [2010] suggested that this conundrum might be resolved if the temporal prevalence of IC lightning varied with altitude, speculating a shift to higher altitudes as the storm progresses. This hypothesis requires that the TGFs observed by RHESSI represent those originating at higher altitudes, and therefore retain a detectable intensity at LEO.

1.5. Objectives and Scope

[25] This study identifies candidate source lightning events. These events are used to obtain an improved profile reflecting the distances of source discharges from the subsatellite point, explore the temporal relationship between TGFs and the causative lightning and provide evidence supporting a power law distribution for TGF intensities.

2. Data

2.1. TGF Data

[26] RHESSI was launched on 5 February 2002 into a circular orbit at a nominal altitude of 600 km. The orbital inclination of 38° spans the zone of principal lightning activity, although RHESSI does not record data within the South Atlantic Magnetic Anomaly (SAMA) or at high magnetic latitudes. RHESSI's detectors are sensitive to photon energies from ~3 keV up to 17 MeV, and are effectively omnidirectional but retain no direction information [*Smith et al.*, 2002b].

[27] RHESSI's altitude determines its geometric Field of View (FOV), which extends to $\alpha_{max} \approx 66.7°$ ($x = 2590$ km). The detection efficiency is not uniform across the FOV but peaks at nadir and plummets as α approaches the horizon. TGFs close to the horizon are effectively undetectable. Consequently, a somewhat smaller effective FOV is assumed to extend out to only $\alpha = 60°$, which corresponds to a distance of 1170 km from the nadir point, covering an area of around 4.3 Mm^2 on the ground.

[28] The complete RHESSI data are telemetered to the ground for offline analysis and are thus not limited by a trigger threshold. These raw data are subjected to a TGF search algorithm [*Grefenstette et al.*, 2009] designed to minimize the occurrence of false positives. The resulting TGF catalogue is thus not complete, but unlikely to contain spurious events.

[29] The primary objective for RHESSI was to examine solar flares, but its capabilities also permit the detection of TGFs. However, the time scales of solar flares are ~1 s, so that RHESSI was not designed to achieve the stringent timing accuracy required for TGF analysis. Since the duration of a typical TGF is only a few 100 μs, it is generally not possible to assign a time to a particular event with much better than 0.1 ms precision. In addition, since TGFs identified by RHESSI contain on average only 25 photon counts, marginally above the detection threshold, the construction of a robust algorithm for assigning the onset time of a TGF is extremely difficult (B. W. Grefenstette, private communication, 2010). RHESSI TGF times are thus presented with only 1 ms precision.

[30] A fortuitous joint observation of magnetar SGR 1806-20 by both Swift and RHESSI on 27 December 2004 indicated that the RHESSI clock was in error. An absolute correction of +1.8 ms was consequently applied to all RHESSI data [*Grefenstette et al.*, 2009] and is included in the analysis presented here. Due to uncertainty in the latency incurred in the communication between RHESSI and ground stations, this correction, which is based on only a single observation, may not be definitive and might vary through the mission. *Connaughton et al.* [2010b] demonstrated a drift in the RHESSI clock, so that a constant offset is not strictly applicable. As a result, even the corrected RHESSI TGF times should be regarded as having an uncertainty of around 1–2 ms. Investigation of the causal relationship between TGFs and lightning using RHESSI data is thus fraught with ambiguity.

2.2. Lightning Data

[31] Direct associations between TGFs and specific, well characterized lightning discharges would elucidate the present understanding of TGFs. Some previous studies have used arrival time and azimuth of Very Low Frequency (VLF) sferics observed from a single location [*Inan et al.*, 1996; *Cummer et al.*, 2005; *Cohen et al.*, 2006]. *Cohen et al.* [2010] used sferic observations from two or more AWESOME VLF receivers to triangulate the location of possible source discharges. A number of other studies [e.g., *Hazelton et al.*, 2009; *Smith et al.*, 2010] have used lightning data from the World Wide Lightning Location Network (WWLLN).

[32] WWLLN [*Dowden et al.*, 2008] uses the VLF radio burst, or sferic, produced by a lightning stroke to triangulate the discharge location. Since the attenuation is low at VLF, WWLLN is able to detect global lightning activity with only a limited number of receivers [*Dowden et al.*, 2002, 2008; *Lay et al.*, 2004]. The temporal and spatial accuracies of the network are ~30 μs and <10 km respectively [*Rodger et al.*, 2005; *Jacobson et al.*, 2006]. The WWLLN event times correspond to the times of peak energy release.

[33] A number of quirks which characterise the WWLLN data had to be accounted for in this analysis (R. H. Holzworth, private communication, 2010; J. B. Brundell, private communication, 2010). The algorithm for grouping sferics from different sets of WWLLN stations can sometimes result in a single lightning discharge being identified independently by two disjoint sets of stations. This redundancy arises from the WWLLN location algorithm attempting to group data from as many stations as possible (at present up to 20 stations may identify the sferic from a given lightning stroke) to improve location accuracy while at the same time neglecting spurious events from noisy stations and events with seren-dipitous timing. Efforts are being made to mitigate these aberrations in the raw WWLLN data, but for the present study, duplicate events which differed in location by <20 km and time by <1 ms were removed. Although WWLLN is capable of identifying distinct but effectively simultaneous events, separated in time by just ~1 μs, the contribution of individual stations to these events is limited by the minimum trigger period of 1.3 ms per event per station since it is not feasible to untangle the signals from more than one sferic within this interval. Events in the WWLLN data may also occur slightly out of sequence as a result of the grouping technique used in the location algorithm. This is easily rectified during post-processing. It should be noted, how-ever, that collocated WWLLN events which are separated by a few 10 ms are probably multiple strokes from a single lightning flash.

[34] The fidelity of the WWLLN locations is assured by insisting that the timing residual be less that 30 μs and that at least five stations identify a particular sferic. This constraint was applied to all of the WWLLN data used in this analysis. It is, however, feasible to uniquely identify lightning loca-tions based on only four stations. This can increase the number of events detected but will also proliferate the pro-portion of spurious events. Therefore, events identified under these relaxed constraints need to be validated assid-uously and such an analysis is thus only practicable for limited periods of data [*Connaughton et al.*, 2010a].

[35] *Lay et al.* [2004], in a case study of lightning over Brazil during the infancy of WWLLN, observed that the mean peak current of WWLLN events was between 70 and 80 kA. *Dowden et al.* [2008] later found that strokes with peak current less than 25 kA were seldom identified by WWLLN. The apparent peak current threshold resulted in a global detection efficiency of ~5–6% for all lightning strokes and ~15% for CG strokes [*Rodger et al.*, 2009a]. Despite the relatively low efficiency, comparisons of WWLLN with other lightning detection systems has estab-lished that it is representative of global lightning activity [*Jacobson et al.*, 2006].

[36] WWLLN is capable of identifying both CG and IC lightning discharges, but does not distinguish between them [*Lay et al.*, 2004; *Rodger et al.*, 2005, 2006]. The coinci-dence algorithm employed by WWLLN is biased towards more vigorous lightning discharges with higher peak cur-rents [*Jacobson et al.*, 2006; *Lay et al.*, 2007; *Rodger et al.*, 2009b]. As a result it appears that WWLLN is considerably more sensitive to CG discharges [*Lay et al.*, 2007] which generally have higher peak currents. In a comparison of WWLLN to a local lightning detection network in Australia, *Rodger et al.* [2005] found the efficiency of WWLLN to be ~26% for CG and ~10% for IC strokes. *Jacobson et al.* [2006], in a Florida case study, observed that ~26% of the WWLLN events corresponded uniquely to Los Alamos Sferic Array (LASA) [*Smith et al.*, 2002a] IC discharges. A considerable proportion of the ICs identified by WWLLN are likely to be Narrow Bipolar Events (NBEs), which are the only class of IC discharge having currents exceeding 30 kA.

[37] WWLLN is an experimental network and since its inception the triggering techniques used to identify sferics, the algorithm used to assimilate the sferic data and the number of receivers have improved, resulting in consistent enhancements in sensitivity to lightning with lower peak currents and a consequent increase in the total number of lightning strokes reported [*Rodger et al.*, 2009b]. A number of specific events during its evolution have had a profound influence on the quality of the data. WWLLN initially located lightning on the basis of station trigger times, with the consequence that locations could be in error by more than 100 km (R. H. Holzworth, private communication, 2010). An improved algorithm based on Time of Group Arrival (TOGA) [*Dowden et al.*, 2002] was implemented from 1 August 2003 [*Rodger et al.*, 2005]. In February 2006 the average number of data packets per second sent by each station was reduced from five to three, which resulted in a further increase in the number of strokes located. The location algorithm and management protocol for WWLLN are still being regularly updated. The raw TOGA data packets, which have been archived since August 2004, are occasionally reprocessed using the refined algorithm, which has improved the accuracy of the lightning locations and removed some artifacts from the data.

[38] From 2005 to 2009 the total number of discharges identified by WWLLN rose from 39 to 115 million per year. This has also been associated with appreciable progress in detection efficiency when contrasted with regional com-mercial lightning detection networks. For example, com-parison of WWLLN data with the New Zealand Lightning Detection Network (NZLDN) over the same period shows
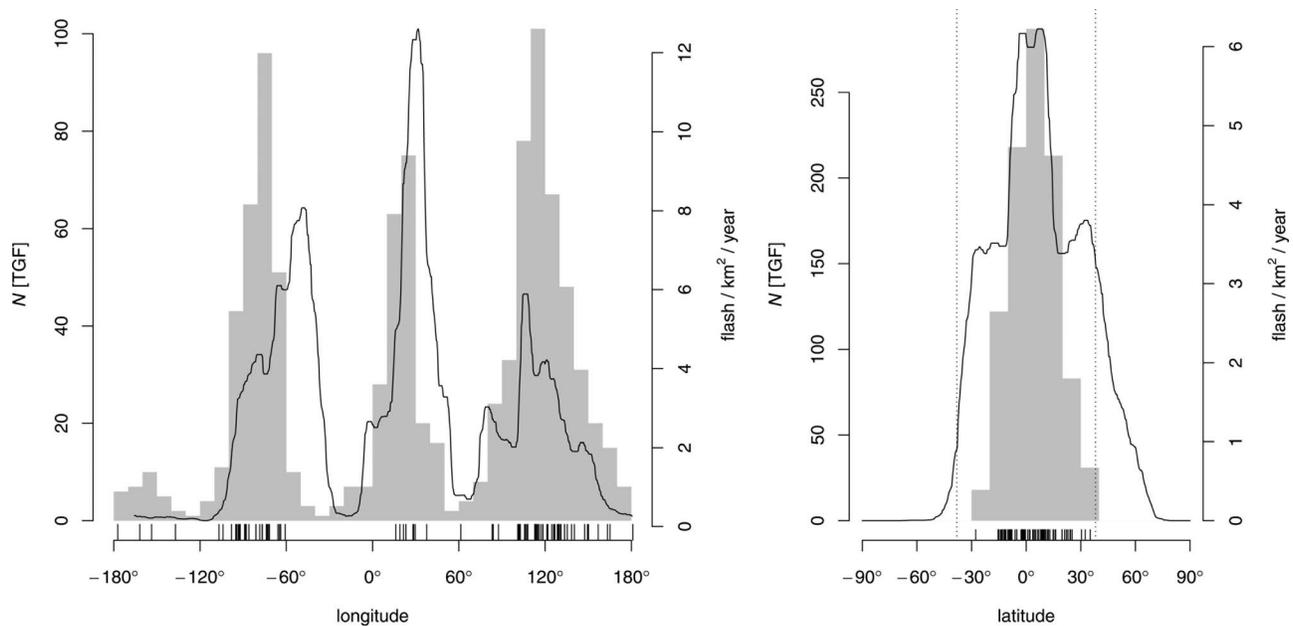
Figure 2. Geographic distribution of the 972 TGFs identified by RHESSI between 4 March 2002 and 6 September 2010 (histogram) compared to the lightning distribution derived from the LIS/OTD High Resolution Full Climatology (HRFC) version 2.2 gridded data (line). The HRFC data were weighted by the cosine of latitude when creating the zonal profile. The orbital inclinations for OTD and LIS are 70° and 35° respectively. The locations of lightning strokes coincident with TGFs are indicated by a rug of ticks. The TGF peak over the Americas is offset to the west of the lightning peak because RHESSI does not observe through the SAMA. The vertical dotted lines in the latitude plot reflect the extremities of the RHESSI orbit.

detection efficiencies have improved from 3.3% to 18.3% for all lightning, and from 12.7% to 46.7% for intense lightning discharges (absolute current >50 kA) (C. J. Rodger, private communication, 2010). *Abarca et al.* [2010] compared WWLLN data over the contiguous United States between 2006 and 2009 to the corresponding National Lightning Detection Network (NLDN) data, finding that the detection efficiency for CG discharges improved from 3.9% to 10.3%, and confirmed the relationship of detection efficiency to lightning peak current. In contrast the IC detection efficiency changed from only 1.78% to 4.82% during the same interval. For the most powerful CG discharges, *Abarca et al.* [2010] found that the detection efficiency was as high as 35%.

[39] Although WWLLN provides continuous global lightning coverage, its efficiency varies with both location and time, and it is thus not capable of generating accurate measurements of the absolute density or rate of lightning discharges. The detectors on the Optical Transient Detector (OTD) and Lightning Imaging Sensor (LIS) satellites, by contrast, are able to provide accurate measurements of flash rate densities but, due to the nature of satellite observations, these are necessarily limited in both space and time. These gridded LIS/OTD data are used for comparison with the global distribution of TGFs.

3. Analysis and Results

[40] The list of TGFs used in this analysis is based on the catalogue of *Grefenstette et al.* [2009], which presents TGF times along with the corresponding geographic coordinates

of RHESSI. The extended catalogue lists 972 TGFs between 4 March 2002 and 6 September 2010. The altitude of RHESSI averaged over the observed TGFs was $\langle z \rangle = 564.7 \pm 0.4$ km.

3.1. General Distribution

[41] The geographic distribution of the RHESSI TGFs is compared to the climatological distribution of global lightning activity in Figure 2. It is apparent that TGFs are most commonly observed close to the equator. The distribution declines rapidly with increasing latitude, while lightning activity has a shoulder which extends into the subtropics. *Smith et al.* [2010] found that this discrepancy could be partially accounted for by the effect of atmospheric absorption, where the elevated tropopause at low latitudes results in higher thunderclouds. Including the effects of RHESSI exposure and γ-ray attenuation from the tropopause to LEO yields improved agreement between the TGF and lightning distributions [*Smith et al.*, 2010, Figure 6]. The latitudes of the observed TGFs extend from 29.4°S to 38.0°N. The latitudinal asymmetry is partly due to the fact that RHESSI does not operate within the SAMA, but the latitudinal extent of the source lightning and RHESSI's orbital inclination may also be influential. Orbital inclination is not a limitation in the Southern Hemisphere, where the decrease in lightning occurrence south of 30°S is more dramatic. It is, however, possible that some Northern Hemisphere TGFs are not being detected since they fall outside the orbital range of RHESSI. However, this is unlikely to represent a significant number of events.

[42] The longitudinal distribution reflects the zonal pattern of lightning occurrence, with peaks over the three major tropical chimney regions [*Williams and Sátori*, 2004]. If one considers three longitudinal zones then, of the 972 TGFs, 436 were observed over Asia and the Maritime Continent (60°E to 180°E), 283 over the Americas (120°W to 40°W) and 216 over Africa (20°W to 50°E). *Splitt et al.* [2010] found that TGFs were appreciably more common over land and coastal areas than over the oceans, although the presence of numerous small bodies of land in the Maritime Continent resulted in an elevated TGF count in this essentially oceanic domain. *Smith et al.* [2010] identified TGF deficits over Africa, the United States and Asia, suggesting that regions proximate to the oceans are most conducive to TGFs. Despite the fact that global lightning activity is most profuse over Africa [*Christian et al.*, 2003], the smallest number of TGFs have been observed in this zone. It is possible that the relative paucity of RHESSI TGFs over Africa, in particular, might be due to the deadtime suppression of brief but intense events, where the detector is unable to accumulate the required number of counts [*Smith et al.*, 2010]. This explanation might not be plausible in light of the numerous Compton scattered photons likely to be present in the delayed tail of such an event. Another explanation might be found in provisional results which indicate that the relative proportion of powerful lightning discharges over Africa is lower than that over the other two tropical chimneys [*Reeves et al.*, 2010].

[43] The distributions presented in Figure 2 are based exclusively on TGFs detected by RHESSI, and are thus limited by its finite sensitivity and FOV. RHESSI is unable to detect TGFs occurring outside its FOV, TGFs with low intrinsic brightness or TGF sources too deep in the atmosphere. The true global rate and distribution of all TGFs is currently unknown although, based on a global lightning flash rate of 44 ± 5 s^{-1} [*Christian et al.*, 2003], *Smith et al.* [2011] have estimated the global TGF frequency as ~10 min^{-1}.

[44] TGFs are most common during the local afternoon [*Splitt et al.*, 2010], which is consistent with the diurnal pattern of lightning over land. Greater insight might be achieved by considering the solar zenith angle at the time of the TGFs. On a seasonal scale, the number of TGFs identified during the Northern Hemisphere summer (July to August), $N_S = 272$, exceeds that during the Southern Hemisphere summer (December to February), $N_W = 173$. This bias is somewhat surprising in light of the fact that the African source is confined south of 15°N due to the dearth of lightning over the Sahara Desert, but probably arises from the absence of data over the SAMA. *Christian et al.* [2003] noted that the global lightning rate varied between $R_S = 55$ s^{-1} in Northern Hemisphere summer and $R_W = 35$ s^{-1} during Southern Hemisphere summer. It is interesting to observe that the ratio of the TGF counts in these two seasons ($N_S/N_W = 1.572$) is consistent with the ratio of the rates determined by *Christian et al.* [2003] ($R_S/R_W = 1.571$), although the close correspondence is likely to be coincidental.

3.2. Geolocation Algorithm

[45] Using WWLLN data it is possible to link individual TGFs to plausible source lightning discharges. For each TGF the WWLLN data were filtered to extract events which

occurred within a 20 min window centered on the TGF epoch and less than 2400 km from the RHESSI nadir. The times of this subset were corrected for time of flight to RHESSI, assuming a source altitude of $h = 20$ km. Uncertainty in the production altitude does not significantly influence the time of flight calculations. The vacuum speed of light was employed, which is a valid assumption for the most energetic photons, but is less applicable for dispersed photons which have undergone multiple scattering events. It is thus suitable when $\alpha < \theta$, but may induce a small bias when $\alpha > \theta$. Of the filtered events, those falling within a 20 ms window centered on the TGF epoch were retained as candidate matches. The width of this window is sufficient to allow for propagation from the periphery of the RHESSI FOV as well as allowing for uncertainties in timing. According to these criteria, 93 of the 972 TGFs had WWLLN matches, corresponding to a match rate of only 9.6%. Once the matches had been identified it was possible to determine their distance from the RHESSI subsatellite point. The 2 matched lightning discharges which were further than 1200 km were discarded. Both of these events had brief time profiles and were thus not considered to be possible electron events.

[46] The number of coincident TGFs identified over Asia and the Maritime Continent, the Americas and Africa are 52, 27 and 9 respectively. The locations of these events are indicated by a rug of ticks in Figure 2. The proportions of matched events is not in keeping with the proportions of observed events in these longitudinal zones, but may reflect the fact that the efficiency of WWLLN is highest over the Maritime Continent and lowest over Africa.

3.3. Chance Coincidences

[47] To make an assessment of the probability of chance coincidences, one must estimate the average lightning rate within the RHESSI FOV. From the LIS/OTD HRFC data the maximum flash rate density within the RHESSI orbit is 153.3 km^{-2} yr^{-1}. The highest possible flash rate within the effective RHESSI FOV is thus 20.9 s^{-1}. Assuming that lightning is a Poisson process, the intervals between flashes should be described by an exponential distribution. Employing the maximum possible flash rate to evaluate the Cumulative Distribution Function (CDF), one finds that the probability of a lightning flash occurring by chance in the RHESSI FOV within an arbitrary 20 ms interval is $P = 0.34$. Since the maximum flash rate density was assumed in this calculation, this constitutes a highly conservative result. A more realistic assessment might be obtained by taking the 95% quantile of HRFC flash rate density, 20.9 km^{-2} yr^{-1}, which yields a flash rate of 2.8 s^{-1} within the RHESSI FOV and a probability for chance coincidence of $P = 0.06$. On the basis of global lightning frequency, there is thus a finite probability of chance coincidence. However, according to the binomial distribution, obtaining 93 chance matches out of 972 TGFs has the trifling probability of $P = 1.6 \times 10^{-7}$, which is very improbable indeed.

[48] The above calculations were based on average lightning rates. Lightning activity varies both spatially and temporally, so it is more meaningful to estimate the probability of a chance coincidence using lightning data applicable to the time and location of a given TGF. Since the WWLLN events within a 20 min window centered on each

longitude: 20.29°
latitude: 9.81°
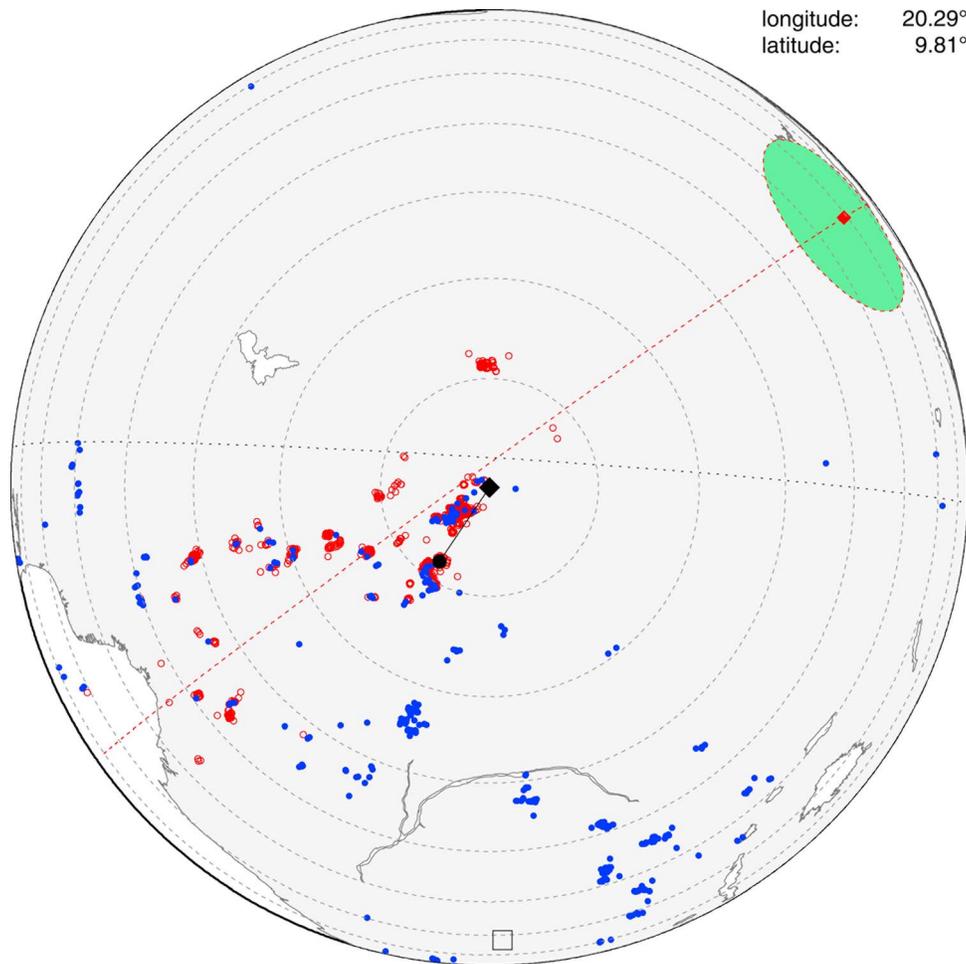
Figure 3. Locations of WWLLN (blue) and LIS (red) lightning during the 20 min period centered on the 4 October 2005 (17:18:59.707 UTC) TGF. RHESSI was located at an altitude of 553 km above 9.81°N 20.29°E as indicated by the central black diamond. The concentric dashed circles indicate distances from the RHESSI nadir at intervals of 300 km. The extent of the plot corresponds to the RHESSI FOV. The magnetic footpoint of the field line passing through RHESSI is denoted by the black square. The location of the causative lightning stroke at 8.0°N 19.0°E is indicated by a black dot which is linked to RHESSI by the black great circle path. The path of LIS during the 20 min interval is reflected by the dashed red curve and the approximate LIS FOV at the time of the TGF is represented by the green shaded circle.

TGF were retained, it was possible to individually assess the probability of a chance match. Assuming that the lightning events were uniformly distributed in time would be overly conservative since it would not take into account clusters of strokes. Therefore, a simple Monte Carlo procedure was used to provide a more realistic evaluation. This procedure examined a large number of 20 ms intervals chosen at random close to the TGF epoch and estimated the proportion which contained lightning events. A similar technique was employed by *Briggs et al.* [2010] and *Connaughton et al.* [2010a], although they used 10 ms test intervals and selected them in a more systematic way. Although the probability of chance coincidences varies between TGFs due to changes in the frequency and distribution of WWLLN activity, the independent uniform and probabilistic estimates are roughly consistent with each other for any given TGF. The probabilities for a chance match range from 0.011% to 2.6%, with a median of 0.38%, indicating the likelihood of

a false positive is small and the TGF-lightning correlations can be considered statistically significant.

3.4. Example Events

[49] Figure 3 presents the distribution of lightning identified by WWLLN and LIS during the 20 min window centered on the 4 October 2005 (17:18:59.707 UTC) TGF. The agreement between the WWLLN and LIS data validates the efficiency and accuracy of WWLLN in this region at the time of the TGF. The matched WWLLN event, identified by 8 stations with a residual of 21.9 μs, occurred at a distance of 246 km from the RHESSI nadir, at a bearing of 214.0°.

[50] In contrast, Figure 4 illustrates a case where, despite the well defined storm systems within a few hundred km of the RHESSI nadir, no match was found in the WWLLN data. This TGF also does not display the expected signatures of an electron event. Again the similarity between WWLLN and LIS locations endorses the local operation of WWLLN.

longitude: -81.64°
latitude: 4.38°
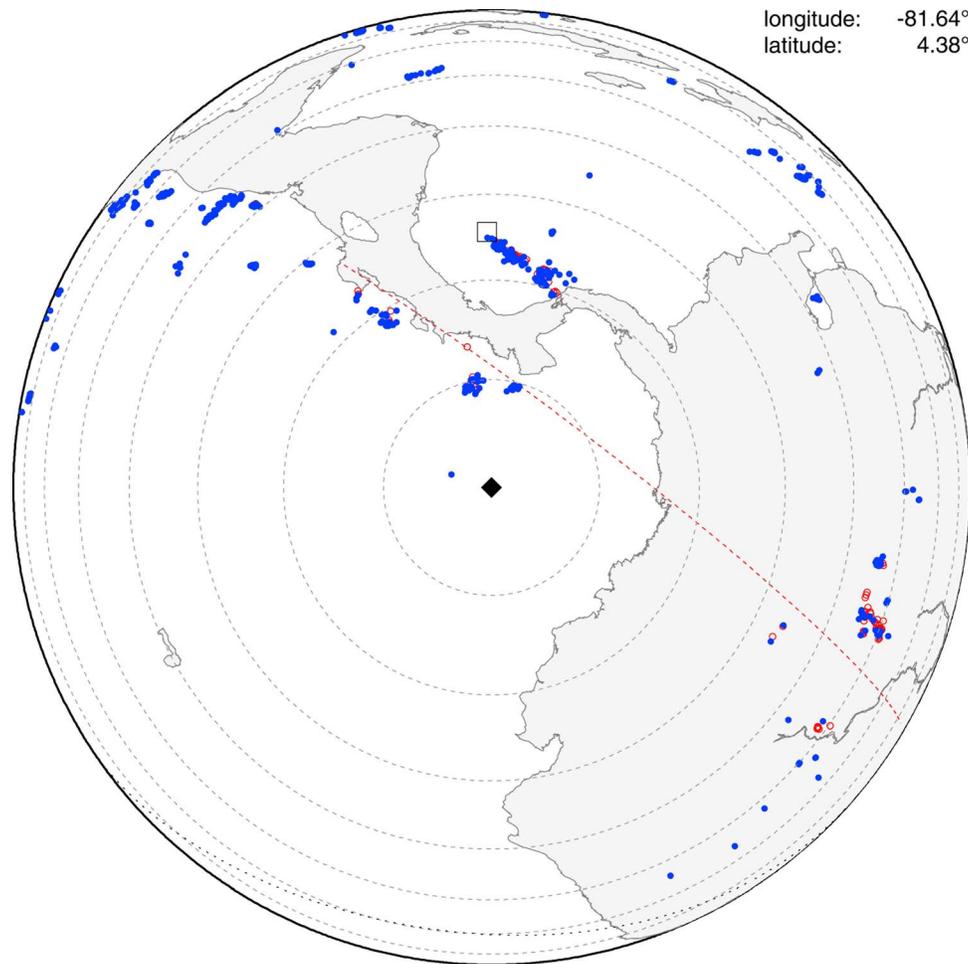
Figure 4. Lightning distribution for the 26 July 2007 (12:10:45.115 UTC) TGF. RHESSI was located at 4.38°N 81.64°W. Format is the same as Figure 3.

Failure to find matching events in lightning data is by no means uncommon. *Inan et al.* [2006] presented two TGFs which were not matched to sferics, despite there being frequent sferics originating from their vicinity, concluding that the TGFs either occurred without lightning or with only very weak lightning. *Cohen et al.* [2006] and *Inan et al.* [2006] indicated that numerous TGFs have been observed above active thunderstorms but without a specific matched sferic, although a portion of these events have subsequently been classified as statistical anomalies [*Cohen et al.*, 2010]. *Shao et al.* [2010] found that the majority of RHESSI TGFs were not matched to LASA lightning, suggesting that the causative discharges were below the LASA detection threshold.

[51] Table 1 compares a selection of matched WWLLN events identified in this analysis to those found by *Shao et al.* [2010] (using LASA data), *Cohen et al.* [2010] (using AWESOME data) and *Lu et al.* [2011]. The events identified by *Shao et al.* [2010] were IC lightning with peak currents <10 kA, indicating that WWLLN is capable of detecting relatively weak IC discharges. *Hazelton et al.* [2009] identified the LASA locations for the 11 September 2006 and 16 June 2007 events as being more than 300 km from the sub-satellite point.

[52] While it is apparent that there is reasonable agreement between the *Shao et al.* [2010] and WWLLN loca-

tions, the events on 17 September 2006 and 16 June 2007 are particularly compatible. The agreement for the 11 September 2006 event, however, is relatively poor. This event was matched with a WWLLN stroke over Central America at a distance of 193 km ($\alpha = 19.8°$) and a LASA event at a distance of 371 km. This TGF was also considered by *Cohen et al.* [2010], who related it to a lightning discharge close to the WWLLN match, pointing out that the LASA location for this event might be erroneous due to poor LASA coverage of Central America. In contrast, the TGF on 16 June 2007 which the present analysis associates with lightning at a distance of 362 km ($\alpha = 33.9°$), was matched with lightning at a similar distance of 373 km by *Shao et al.* [2010]. The disparity between the distances from the RHESSI footpoint to the AWESOME and WWLLN matches for the 18 October 2008 is quite acceptable in light of the uncertainties, which are 60 and 30 km respectively. Furthermore, the AWESOME error ellipse for this event includes the WWLLN location.

3.5. Matches Versus Time

[53] Table 2 compares the number of TGFs identified by RHESSI per year to the percentage of TGFs which achieved matches in the WWLLN data. A dramatic change in both statistics occurs after 2006. This can be attributed to two

Table 1. Comparison of Lightning Matches Found by *Shao et al.* [2010], *Cohen et al.* [2010], and *Lu et al.* [2011] With the Corresponding Matches in WWLLN[a]

Date and Time	*Shao et al.* [2010]	*Cohen et al.* [2010]	*Lu et al.* [2011]	WWLLN
11/09/06 04:17:08.478	19.35°N 96.90°W (371 km)	16.41°N 98.03°W (185 km)		16.2°N 98.1°W (193 km)
17/09/06 09:19:34.804	11.60°N 77.58°W (160 km)			10.8°N 76.9°W (268 km)
16/06/07 20:16:57.846	14.95°N 92.26°W (373 km)			14.9°N 92.1°W (362 km)
18/10/08 21:55:38.392		9.81°N 72.86°W (207 km)		9.7°N 73.3°W (170 km)
05/10/09 04:08:51.843		30.51°N 93.53°W (307 km)	30.40°N 93.42°W (320 km)	30.4°N 93.4°W (315 km)

[a]*Cohen et al.* [2010] locations were only included for events where three or more AWESOME stations contributed. Distances from the lightning location to the RHESSI sub-satellite point are given in parentheses.

possible causes. The reduction (roughly half) in the number of TGFs after 2006 is surely related to the decrease in RHESSI sensitivity caused by radiation damage [*Grefenstette et al.*, 2009]. During 2006 there was also a dramatic increase in the absolute number of events identified by WWLLN. This would probably account for the increase in the percentage of TGFs linked to WWLLN events, provided that the change in WWLLN efficiency resulted in either improved coverage over TGF source regions or the detection of a greater proportion of lightning capable of generating TGFs. Conversely, it is possible that the radiation damage might have biased RHESSI towards TGFs originating from the high peak current lightning generally observed by WWLLN.

[54] Table 2 also reflects the average number of photons detected per TGF, which exhibits a steady decline with time until 2006 when it decreases abruptly. The gradual decrease may be attributed to the cumulative effects of mild radiation damage, while the larger change in 2006 is probably due to severe radiation damage.

3.6. Radial WWLLN Activity

[55] To assess whether the quantity or distribution of lightning activity affects the likelihood of achieving a match, Figure 5 presents the average WWLLN activity during a 20 min period centered on the TGF epoch as a function of distance from the RHESSI nadir. It is evident that irrespective of whether or not a match was found in the WWLLN data, the lightning activity is more vigorous in the vicinity of RHESSI than at larger distances. Further away the activity approaches a limit corresponding to the background level, which is independent of TGF occurrence. From Figure 2 the average flash rate over the range of latitudes covered by RHESSI is 4.1 km^{-2} yr^{-1}. There are on average around 2 lightning strokes per flash [*Watkins et al.*, 2001; *Orville and Huffines*, 2001], so that this translates into an average stroke rate of roughly 8.2 km^{-2} yr^{-1}. Finally,

Table 2. Number of TGFs Identified by RHESSI per Year, N, Average Number of Photons per TGF, $\langle n \rangle$, and the Percentage of the TGFs Which Were Matched by a WWLLN Event

Year	N	$\langle n \rangle$	Match (%)
2002	110	27.6 ± 0.9	3.6
2003	144	26.9 ± 0.8	6.2
2004	156	26.2 ± 0.8	7.7
2005	181	25.6 ± 1.0	6.1
2006	135	23.5 ± 0.9	7.4
2007	79	25.4 ± 1.0	15.2
2008	84	23.4 ± 0.8	16.7
2009	30	22.8 ± 2.3	26.7
2010	53	24.3 ± 1.6	24.5

assuming 15% efficiency for WWLLN [*Rodger et al.*, 2009a], gives a background rate of 1.2 km^{-2} yr^{-1} for WWLLN strokes. This is the rate of WWLLN events per unit area averaged over RHESSI latitudes including areas both with and without storm activity. In Figure 5 the stroke rate at a great distance from the RHESSI sub-satellite point is comparable to this background rate.

[56] Regardless of whether or not a WWLLN match is found for a given TGF, it is apparent from Figure 5 that, relative to the average background level, enhanced lightning activity is detected in the vicinity of the RHESSI sub-satellite point. This is to be expected since TGFs are generally observed above thunderstorms. However, apart from directly beneath the satellite the lightning activity is consistently more intense for matched TGFs. This might indicate that in the case of matches either (i) there is a higher level of lightning, or (ii) the efficiency of WWLLN is higher near to the RHESSI sub-satellite point. Certainly it is well known that WWLLN efficiency exhibits both spatial and temporal
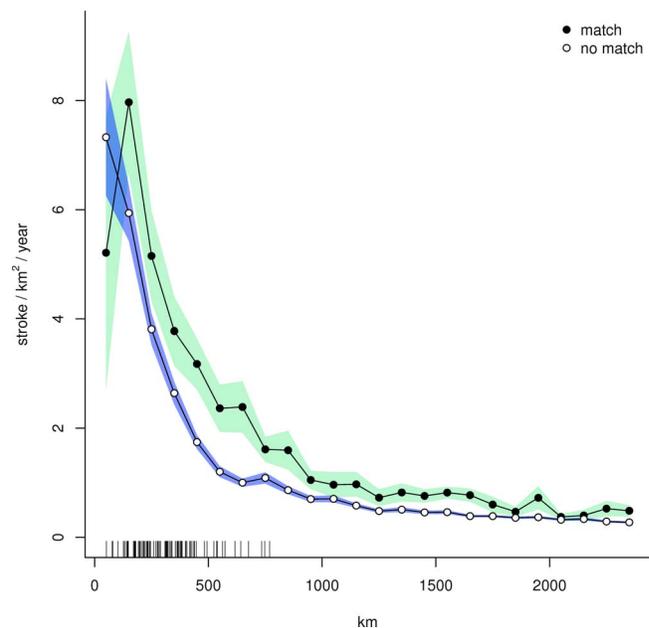
Figure 5. Average WWLLN activity in a 20 min window centered on the TGF epoch as a function of distance from the RHESSI nadir in the case of (•) match or (○) no match between WWLLN and the TGF. The shading indicates the confidence interval corresponding to one standard deviation of the mean. A rug beneath the plot indicates the distances to the matched WWLLN events.

(a)

(b)
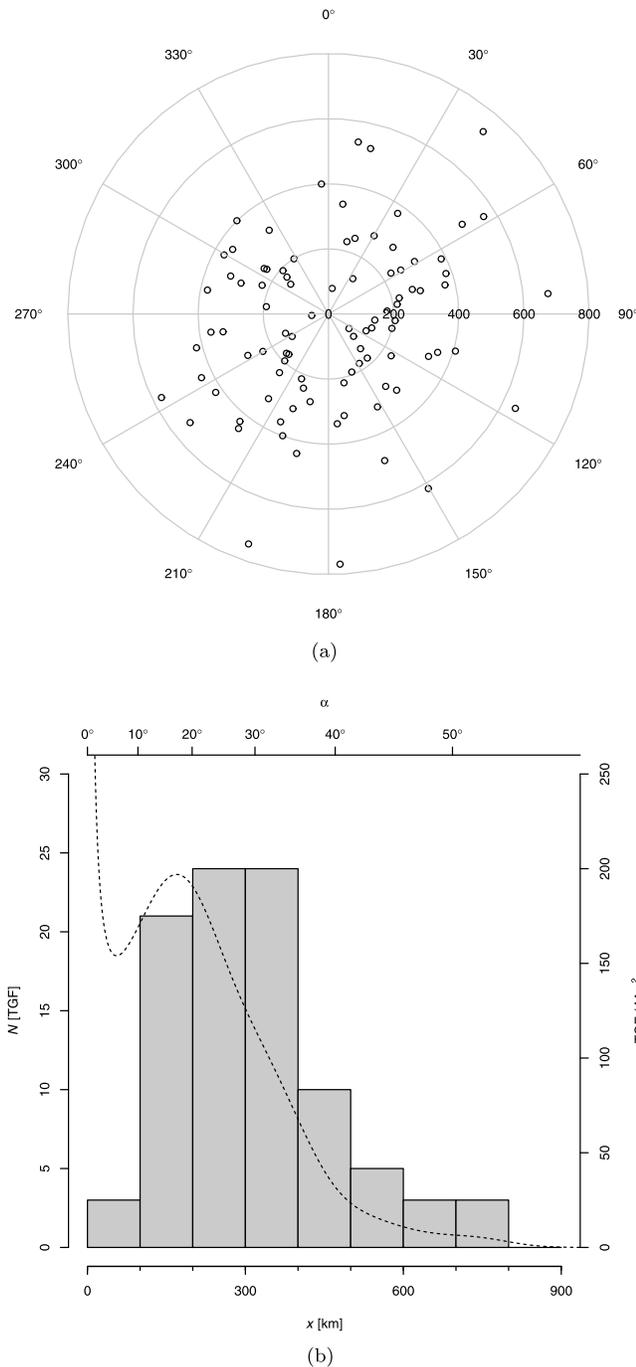
Figure 6. Distribution of distances between RHESSI nadir and matched WWLLN lightning events (a) as a function of bearing from RHESSI and (b) grouped by distance and nadir angle, α. The histogram in Figure 6b reflects the number of TGFs in each distance bin, while the dashed curve is the density of observed TGFs per unit area.

variations. When the data were partitioned into TGFs which occurred over the Americas, Asia and the Maritime Continent, and Africa, the distributions for the former two regions were similar to Figure 5, with the activity for matched events exceeding that for non-matched events. Conflicting results were obtained for Africa, where the activity for all events was less than the corresponding global values, and the matched

events also had relatively lower levels of activity. This is probably due to the poor WWLLN coverage over Africa.

[57] The fact that the average radial distribution of lightning activity at the time of a TGF is peaked below the satellite and drops off fairly rapidly with distance does not preclude the occurrence of TGF matches at greater distances, however these need to possess higher intrinsic intensity in order to be observable at LEO.

3.7. Distance From RHESSI Nadir

[58] For comparison with the general distribution of lightning activity given in Figure 5, Figure 6 presents the distribution of individual WWLLN matches as a function of distance and bearing from the RHESSI sub-satellite point. The bearing appears to be randomly distributed, in agreement with *Stanley et al.* [2006].

[59] Two competing factors influence the form of Figure 6b: decreasing area at small distances leading to fewer TGFs, while at larger distances increasing area is offset by longer path lengths and thus greater attenuation. If one assumes that TGFs occur with uniform probability per unit area within the FOV, then the number of events at distances between x and $x + dx$ is proportional to x. An ideal detector would thus identify an increasing number of TGFs at greater x. However, due to finite detector efficiency and the substantial decline in photon fluence with increasing x, progressively fewer TGFs are identified at large x and the density of observed TGFs per unit area is not constant but deteriorates with increasing x. At larger α the number of TGFs detected declines rapidly due to a decrease in the number of γ-rays reaching LEO, and the detector threshold thus limits the detected TGFs at large α to only the most powerful events. The peak at small distances in the Figure 6b density curve results from the vanishingly small differential areas and is thus spurious. The density of detected TGFs achieves a peak of 197 Mm^{-2} at 169 km ($\alpha = 17°$) from the sub-satellite point. These data should be compared to *Cohen et al.* [2010, Figure 1], who found roughly half this density of events matched in AWESOME data.

[60] TGFs have been correlated with thunderstorms up to 1000 km from the RHESSI sub-satellite point [*Cohen et al.*, 2010], but most are closer. *Cummer et al.* [2005] concluded that the majority of RHESSI TGFs were observed within ~300 km of the sub-satellite point. *Lay* [2008] found a preponderance of coincident strokes with a separation of less than 400 km, but some as far as ~700 km. *Briggs et al.* [2010] and *Connaughton et al.* [2010a] did not find any TGFs further than 300 km ($\alpha = 28°$) from the Fermi sub-satellite point. However, when the GBM data were analyzed in a mode without a trigger threshold, weaker TGFs were detected at distances up to 800 km (V. Connaughton, private communication, 2011). The high threshold trigger algorithm on Fermi GBM prior to November 2009 discriminated against weaker TGFs, and the relatively high number of photon counts per TGF identified by GBM is thus likely to be a selection effect, which would also bias the distances from the sub-satellite point [*Briggs et al.*, 2010]. Both *Briggs et al.* [2010] and *Connaughton et al.* [2010a] found a match rate with WWLLN of around 30%, although statistics are poor due to a limited number of events. It is possible that the more extreme TGFs identified by GBM correspond to
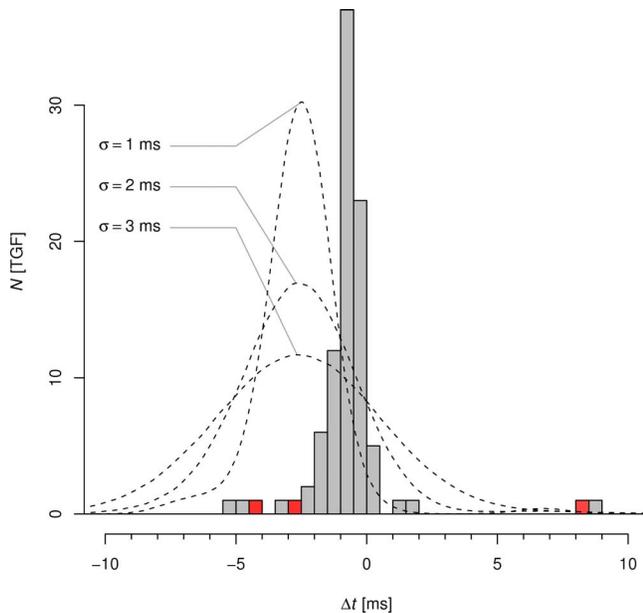
Figure 7. Time delay of TGF with respect to associated WWLLN event (grey), Δt, and next closest WWLLN event (red), $\Delta t'$. Negative Δt indicates that the TGF precedes the lightning stroke. The dashed curves indicate the distributions resulting from removal of the +1.8 ms correction to the RHESSI times, then resampling using random timing errors drawn from normal distributions with standard deviations of 1, 2 and 3 ms.

the high peak current lightning locations from WWLLN. Although others also advocate a nearby source [*Cummer et al.*, 2005; *Stanley et al.*, 2006], there is some evidence of sources at much larger distances [*Lay*, 2008; *Hazelton et al.*, 2009; *Cohen et al.*, 2010]. *Gjesteland et al.* [2011], using RHESSI and model data, have shown that it is possible to observe TGFs at larger α, but that the events must have much greater intrinsic brightness. The constraints developed by *Carlson et al.* [2007] indicate that the observable extent of a TGF at LEO depends on the source altitude, h, and emission width, θ, with observations at larger distances requiring both a broader θ and higher h.

3.8. Time Delay

[61] Figure 7 reflects the statistics of the time delays, Δt, between matched WWLLN events and the corresponding TGFs. The distribution is shifted towards $\Delta t < 0$, suggesting that in the majority of cases, the TGF precedes the associated lightning discharge. The mean delay is −0.77 ms with a 99% confidence interval which extends up to −0.43 ms. A one sided t-test yields $p = 3.5 \times 10^{-7}$, which indicates that the mean delay is significantly less than zero. The delays from the next closest WWLLN events are also indicated and it is evident that there was seldom contention for the best match. The minimum delay for the next closest match is −2.93 ms, while the mean is −793 ms, with a 99% confidence interval which extends from −2.59 to 1.00 s. To place this result into context, *Lay* [2008] found that TGFs preceded the associated WWLLN lightning strokes with Δt = −1.1 ± 1.2 ms. *Cummer et al.* [2005] identified source lightning which appeared to occur subsequent to the TGF,

with an average Δt = −1.24 ± 0.97 ms. *Inan et al.* [2006] observed on average Δt = −0.88 ms. In two case studies, *Stanley et al.* [2006] found that the TGF preceded the associated lightning discharge. *Shao et al.* [2010] found that TGFs preceded the corresponding LASA IC discharges, occurring predominantly during the first few ms of the lightning precursor stage and probably related to pulses during the stepped leader phase. In two case studies, *Lu et al.* [2011] found that TGFs preceded the corresponding lightning discharges by 0.3 and 0.5 ms. These studies, using RHESSI TGF data and lightning data from various sources, all found that TGFs preceded the associated lightning. In contrast, *Cohen et al.* [2006] found that BATSE TGFs occurred 1–3 ms after the causative lightning. More recently, *Cohen et al.* [2010] concluded that the delay between RHESSI TGFs and the causative lightning was not significantly different from zero. *Briggs et al.* [2010], using Fermi GBM data for 12 TGFs, linked 4 TGFs to WWLLN events and found no consistent evidence for precedence between TGFs and lightning. *Connaughton et al.* [2010a], working with an expanded GBM data set of 50 TGFs, found that 13 of the 15 TGFs matched to WWLLN lightning were contemporaneous with the associated discharge to within 40 μs. Two of the *Connaughton et al.* [2010a] TGFs, however, had much larger $|\Delta t| \sim 1$ ms but were still considered to be statistically valid.

[62] The +1.8 ms correction to the RHESSI times was based on a single measurement. It has been suggested that the RHESSI timing error is in fact random. It is thus possible that, rather than redressing the timing error, applied across all events this correction may have introduced a bias. To assess the impact of uncertainty in the RHESSI timing, the correction was first removed from the data. The resulting TGF times preceded the lightning by an even greater margin. The TGFs were then resampled to simulate the correction for random timing errors, where the errors were assumed to be normally distributed with standard deviations of 1, 2 and 3 ms. The resulting distributions are included in Figure 7. If the uncertainty in RHESSI timing is in the order of 1–2 ms, then these results attribute some significance to the $\Delta t < 0$ hypothesis. If, however, the uncertainty is larger, then the observed Δt no longer differs significantly from zero. Finally, comparing the width of the narrow observed distribution to the resampled distributions suggests that if there is a stochastic component to the RHESSI clock drift, then it must be very small, otherwise the observed distribution would be considerably broader.

[63] The uncertainty associated with the RHESSI timing counsels that an attempt to reach any concrete conclusions on the basis of relative timing would be imprudent. Furthermore, a single lightning flash may consist of multiple strokes and it is conceivable that some of the matches used to derive the Δt statistics might not correspond to the actual causative stroke.

4. Discussion

[64] Figure 8 presents the distribution of TGF intensities for the full population of RHESSI events and those which achieved WWLLN matches. The net photon count for each TGF was determined by deducting the average number of background counts from the number of raw counts. For each
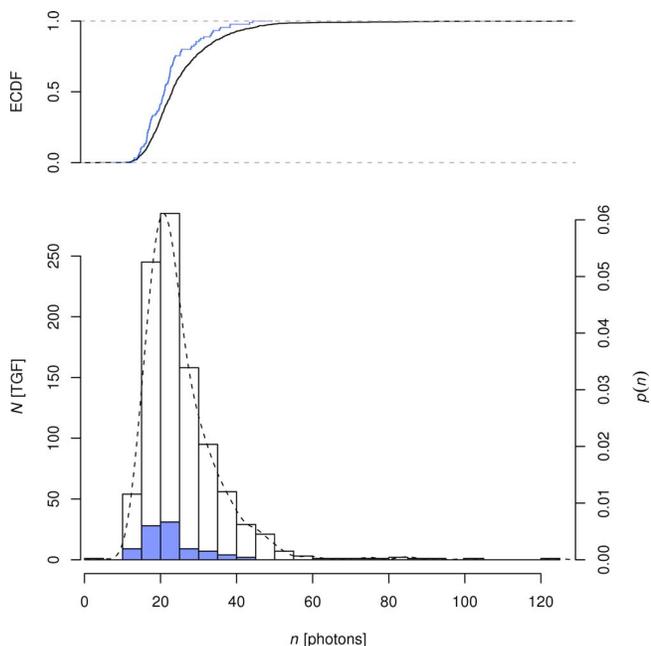
Figure 8. The number of observed TGFs, N, relative to the number of photons per event, n, for all RHESSI TGFs (empty histogram) and TGFs with matches (blue histogram). The dashed curve is the kernel density estimate of the Probability Density Function (PDF) for n. The upper panel reflects the corresponding empirical CDFs.

event the average background photon rate was independently determined. The photon count threshold in the RHESSI search algorithm was applied to the raw photon counts, with the result that some of the events have net counts less than the nominal threshold.

[65] Visual inspection of the histograms in Figure 8 suggests that the distribution of matched TGFs is skewed to the left. Furthermore, the empirical CDF associated with the matched TGFs is consistently higher than that for the whole sample. The difference can be quantified by comparing the empirical CDF for the two distributions using a one sided Two-sample Kolmogorov-Smirnov test. Since both empirical CDFs have ties, it was necessary to employ a bootstrap technique to calculate the correct p-value [Abadie, 2002]. The resulting test statistic is 0.200 with $p = 0.0010$, indicating that the distributions are significantly different at the 1% level and that the distribution of matched events is skewed to lower n. This implies that the WWLLN data, thought to principally contain the most powerful lightning discharges, are more likely to match weaker TGFs. The hypothesis that more intense TGFs are associated with stronger lightning discharges seems to be false, since in this case one would expect the matched events to be prejudiced towards more powerful TGFs. Of course, it is feasible that the relatively poor proportion of matches over Africa may have biased this conclusion. Repeating this analysis for each of the three major regions independently yields $p = 0.0018$, 0.3047 and 0.0334 for Asia and the Maritime Continent, the Americas and Africa respectively.

[66] The form of the upper tails of Figure 8 and Figure 8 of *Grefenstette et al.* [2009] suggest that a power law distribution for TGF intensity is plausible: there is a preponderance of low intensity TGFs, but progressively fewer TGFs with higher photon counts. The cutoff below $n \sim 20$ is a result of finite detection efficiency. Supposing that a power law distribution applies at the source, then the intrinsic number of TGFs, N_0, is related to the number of source photons, n_0, by

$$N_0 \propto n_0^{-k} \tag{1}$$
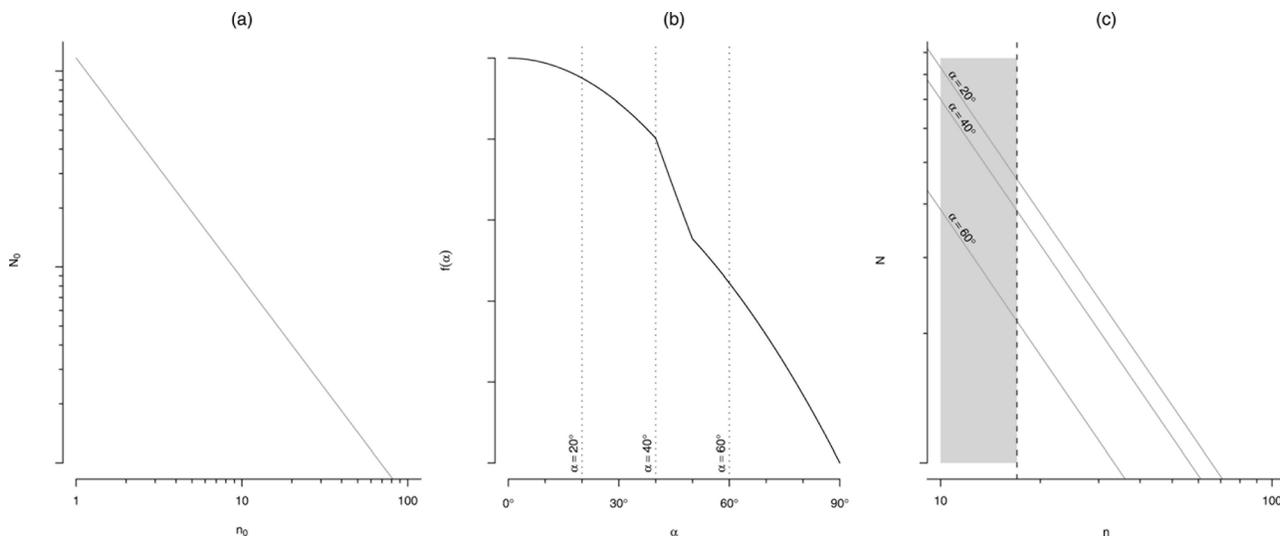
Figure 9. Schematic illustration of (a) the relationship between the intrinsic number of TGFs, N_0, and the number of source photons, n_0; (b) the mapping function, $f(\alpha)$ between the number of source photons and the number of observed photons, n; and (c) the relationship between the number of observed TGFs, N, and n. The knee in $f(\alpha)$ corresponds to the edge of the emission cone. The observation threshold is indicated by the vertical dashed line in Figure 9c, where TGFs with n in the grey shaded region are not detected.
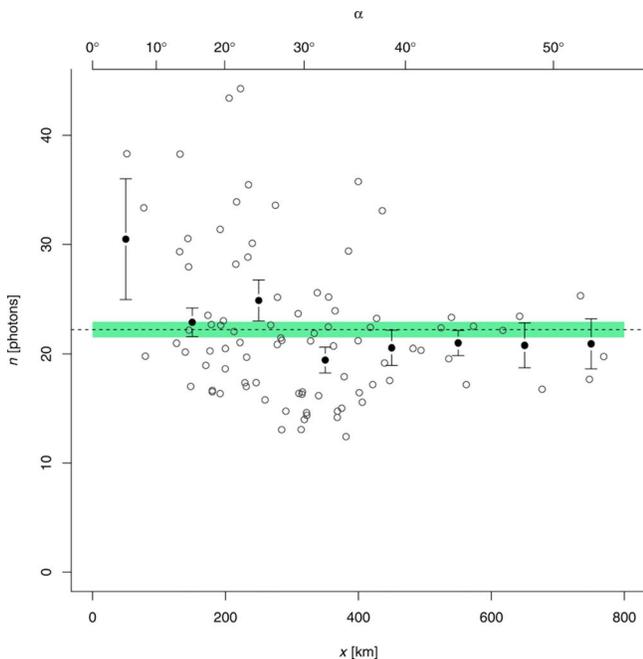
Figure 10. Number of photons per matched TGF as a function of distance from the RHESSI sub-satellite point. Data for individual TGFs (○) are grouped together into distance bins of width 100 km (•). The mean and associated uncertainty for all matched TGFs are represented by the dashed line and shaded region respectively.

with spectral index k. For a given source altitude, the fraction of the source photons which penetrate to LEO can be described by a function, $f(\alpha)$, which depends only on the observation angle, such that the observed number of photons is $n(\alpha) = f(\alpha)n_0$. The magnitude of the scaling function is acutely sensitive to the source altitude. One of the characteristics of a power law distribution is that scaling the argument alters the constant of proportionality but leaves the shape of the distribution intact. The distribution of observed TGFs intensities must thus also follow a power law distribution. These relationships are illustrated schematically in Figure 9. Neither the intrinsic number of TGFs nor the number of source photons is known. RHESSI data reflect only the observed number of TGFs, N, and the associated photon counts, n. Figure 9c also indicates the range of photon counts which fall beneath the RHESSI intensity threshold, where TGFs are no longer detected. The presence of a threshold constrains the domain of applicability of the power law model to those n above the threshold.

4.1. Support for Power Law Model

[67] Figure 10 compares the RHESSI observed net photon counts to the distances from the matched WWLLN locations. Considering the points for individual TGFs, it is evident that both the number of TGFs and the range of photon counts per TGF decrease with increasing source distance. This is consistent with Figure 9c. Furthermore, the upper envelope of the points decreases with increasing source distance, so that the brightest of the more distant events becomes progressively dimmer. As noted by *Connaughton et al.* [2010b], distant TGFs are generally dim, while those

from nearby exhibit a range of intensities. This statement is supported by the power law model, where the range of observed n for $\alpha = 20°$ is appreciably broader than that for $\alpha = 60°$. With increasing α the range of possible n above the threshold gradually diminishes.

[68] Subject to the assumption of a power law relationship between N and n with a threshold, the expected mean number of photons per TGF does not vary with α, but depends only on the spectral index and the threshold value. To determine whether this is reflected in the RHESSI data, mean photon count per TGFs was calculated when the data were grouped together into distance bins of width 100 km. These means are reflected in Figure 10. The individual means should be compared with the number of photons per TGF averaged over all events, 25.5 ± 0.3, and for all matched events, 22.2 ± 0.7. The latter statistic is also indicated in Figure 10. A one way ANOVA test indicates that the differences between the average counts at various distances are not statistically significant ($p = 0.068$). This is confirmation that the expected number of observed photons does not vary with source distance, which lends additional support to the power law model. The marginal p does not, however, provide conclusive evidence for the power law model.

[69] The foregoing analysis does not take into account the possible influence of instrumental deadtime, which would have the greatest impact at small α. Both the number of photons and event duration are important when considering deadtime since they jointly determine the count rate. A large n achieved during a long duration event will have a moderate count rate and is thus unlikely to suffer from deadtime. However, a large number of photons during a short event could incur significant deadtime. TGFs originating close to the satellite are more likely to produce a high γ-ray count rate at LEO and thereby saturate the detector. It is thus quite possible that the number of photons recorded for events at low α underestimates the true count. The influence of this would be a larger mean photon count for small α, which would cast doubt upon the above conclusions.

[70] The distribution functions of numerous processes are suitably approximated by a power law. It has been postulated that a power law distribution with a lower threshold might be applied to TGF observations. Two consequences of the scaling properties of such a distribution are that (i) the range of possible photon counts must decline with increasing observation angle, while (ii) the expected mean photon count should remain independent of the observation angle. Both of these characteristics are observed in the RHESSI TGF data when the observation angle is determined from source locations derived from WWLLN matches. Although these observations support the power law hypothesis, it is unfortunately quite possible to falsely identify a power law [*Clauset et al.*, 2009]. The likelihood of such a misdiagnosis declines with increasing sample size. A more rigorous treatment of this question is planned for a later study.

[71] TGFs are rare events. *Smith et al.* [2011], based on aircraft observations of thunderstorms in which only a single TGF was observed from 1213 lightning discharges, estimated that the ratio of TGFs to lightning flashes is in the order of 10^{-2} to 10^{-3}. The apparent rarity of TGFs suggests that they are produced by lightning discharges with scarce and unique characteristics or that peculiar additional conditions are

necessary. *Lu et al.* [2011], for example, conclude that the mean current required to produce a TGF in an IC leader would be 5–10 kA, which is an infrequent occurrence given that the typical current is <1 kA.

[72] Taken literally, the power law model predicts an enormous number of low intensity TGFs. Naturally such a prediction is quite unphysical and the total number of TGFs must be limited by the quantity of global lightning. One would thus anticipate that some threshold value of n_0 would exist below which N_0 would drop rapidly to zero. Alternatively the distribution may achieve a plateau at low n_0. These possibilities can only be assessed with additional observations from more sensitive detectors.

4.2. WWLLN/TGF Mismatch

[73] Using WWLLN lightning data, source matches were found for 93 of 972 TGFs, a success rate of only 9.6%. Previous attempts to find correspondences between TGFs and lightning have achieved comparable levels of success. *Lay* [2008], for example, found that only 4.3% of TGFs between June 2002 and October 2006 had one or more coincident WWLLN lightning strokes. Coincidences with lightning data from the ZEUS VLF network are also rare [*Chronis and Anagnostou*, 2003; *Williams et al.*, 2006]. One might be tempted to assume that the relatively low efficiency of WWLLN is responsible. The similarity between the success rates and the WWLLN detection efficiency [*Jacobson et al.*, 2006] led *Lay* [2008] to suggest that RHESSI TGFs were produced by lightning strokes with peak current >30 kA.

[74] The average match rate of 9.6% pertains to the entire period from 4 March 2002 to 6 September 2010, during which WWLLN efficiency was consistently escalating. *Connaughton et al.* [2010a] recently achieved a WWLLN match rate of 30% for the 50 TGFs detected by Fermi GBM between July 2008 and March 2010. The discrepancy between these match rates is resolved by referring to Table 2 where it is apparent that from 2007 the RHESSI match rate is significantly higher than the average and comparable to the rate of *Connaughton et al.* [2010a].

[75] The paltry number of coincidences in the WWLLN data may be related to the fact that WWLLN is most responsive to potent CG lightning discharges occurring in the lower atmosphere, while the most likely TGF sources are IC discharges at altitudes in the range 15–20 km. The existence of a finite number of correlations does, however, indicate that WWLLN is detecting some of the causative IC lightning discharges. Furthermore, the match rate of only 9.6% is consistent with the IC efficiency of WWLLN [*Rodger et al.*, 2005]. This may be coincidental. Alternatively it might suggest that if TGFs are indeed produced by IC discharges then the relatively poor correlation between TGFs and WWLLN events could be attributed to the IC detection efficiency of WWLLN.

[76] The radial distribution of WWLLN lightning is similar regardless of whether or not a match was found for a given TGF. The distribution peaks beneath the satellite and declines with increasing radial distance. The levels are slightly elevated in the case of matches. WWLLN thus normally detects enhanced lightning activity in the vicinity of RHESSI at the time of a TGF. The distinction between matched and unmatched events is likely to be related to local variations in WWLLN detection efficiency which, in the case of matches, produce a higher level of lightning activity in the vicinity of RHESSI but also increase the likelihood of capturing the matching lightning discharge.

[77] TGFs which yield matches in the WWLLN data are generally those with fewer photons per TGF. Since WWLLN is biased towards more intense CG lightning, this poses an intriguing possibility. Intense TGFs are probably produced at higher altitude by IC lightning, which is infrequently detected by WWLLN. TGFs which are weaker at LEO are likely to be produced at lower altitudes, possibly by CG lightning which is more susceptible to WWLLN detection. The difference in intensity is related to the degree of atmospheric attenuation, which is linked to lightning source height and hence to the probability of detection by WWLLN. An alternative explanation is that, with the growing efficiency of WWLLN, more TGFs have been matched subsequent to the RHESSI radiation damage, and the lower average intensity of these TGFs has biased the statistics. The analysis presented in Figure 8 was repeated independently for the two sets of TGFs detected before and after the radiation damage, but the conclusion remained the same. The alternative explanation therefore does not appear to be supported by the data.

4.3. TGFs Without Lightning Matches

[78] The copious number of TGFs without lightning matches might be explained by (i) lightning activity near one of the magnetic footpoints generating an electron-positron beam, (ii) lightning that is not detected by WWLLN (low peak current or IC), or (iii) generation without an accompanying lightning discharge. Electron-positron events are readily recognized since their duration is much longer than that of a typical TGF. *Briggs et al.* [2010] discuss the discrimination of electron-positron events based on their duration. It is possible that electron-positron events observed very close to the source or with only a small spread in pitch angles may have a shorter duration. Regardless, option (i) has been eliminated by a detailed examination of the time profiles of each of the events. In the case of option (iii), the process leading to a TGF might completely discharge the potential within a cloud, so that a lightning discharge fails to take place. The ability of the feedback model of RREA [*Dwyer*, 2007] to swiftly neutralize the ambient electric field before it achieves the threshold for conventional breakdown indicates that it is feasible to generate a TGF without lightning. Finally, in support of option (ii), *Inan et al.* [2006] found that a portion of TGFs were not accompanied by a detectable sferic, concluding that an intense lightning discharge is not required for TGF production.

[79] *Cummer et al.* [2005] found that the TGFs which were not clearly connected to a specific lightning discharge did not possess any distinctive characteristics. This suggests that whether or not a match is found is more likely to be a reflection on the lightning data than the particular traits of a TGF. Certainly this analysis does not reveal those characteristics which might result in a match for one TGF but not another, the relationship appearing to be completely unpredictable. Furthermore, if one were to postulate that the capability of pre-discharge processes to generate a TGF were independent of the characteristics (intensity, orientation, polarity) of the subsequent lightning stroke, then this

would support the apparently capricious correlation between TGFs and WWLLN events.

[80] Photons originating in the lower atmosphere are severely attenuated before reaching LEO, placing a threshold on the intrinsic intensity of observable TGFs. Although not all lightning discharges produce observable TGFs, there are currently no TGF observations with irrefutable evidence of the absence of coincident lightning. The finite efficiency of WWLLN leaves open the possibility that lightning did occur but was just not detected. On the contrary, it has been shown that a number of TGFs can be directly connected to individual lightning discharges. Therefore, although the converse is theoretically possible [*Dwyer*, 2007], the hypothesis that all TGF events are produced in association with lightning must still hold.

4.4. TGF Timing

[81] A negative delay, $\Delta t < 0$, indicates that TGFs precede the associated lightning and are thus likely to be generated during the initial stages in the development of a lightning discharge. It has been demonstrated that this conclusion holds under the assumption of a small stochastic error in RHESSI timing.

[82] Some independent studies support the $\Delta t < 0$ conclusion. *McCarthy and Parks* [1985], while flying through a thundercloud, found that X-ray fluxes increased dramatically for ~1 s prior to a lightning discharge but dissipated rapidly thereafter. *Dwyer et al.* [2005] presented evidence to suggest that energetic radiation is liberated prior to a CG return stroke. The emission of X-ray radiation has been observed during streamer formation in laboratory discharges [*Nguyen et al.*, 2008]. The connection between these results and TGFs is, however, tenuous in light of the fact that γ-ray emissions originate from electrons with extremely large kinetic energies, while the electrons which generate X-rays are appreciably less energetic.

[83] Alternative explanations for the negative delay are either a systematic timing offset in the WWLLN or RHESSI data, or an error in the correlation algorithm used in this analysis. Of these the most likely is an error in the RHESSI clock, which is already known to be problematic [*Grefenstette et al.*, 2009].

[84] In contrast, the recent results of *Connaughton et al.* [2010a], derived from the reliable timing on GBM data, suggest that TGFs and lightning are simultaneous to within a few 10 μs. It is probable that the issue of relative timing will only be resolved by data which characterize the detailed temporal evolution of both the TGF and associated lightning discharge.

[85] To this end, the recent study by *Lu et al.* [2011] found that the majority of lightning signals associated with TGFs contained an Ultra Low Frequency (ULF) slow pulse reflecting the transfer of considerable charge over a period of 2–6 ms. The early portion of this pulse is linked to the TGFs and the associated process appears to play an important role in γ-ray production. Single or multiple VLF impulses were superimposed upon the slow pulse. In some instances VLF precursor impulses were observed prior to the slow pulse, but too early to be causally linked to the TGF. The bulk of the charge moment change is driven by the ULF process, while the VLF impulses are produced during small bursts of charge transfer with meagre peak currents [*Lu et al.*, 2011]. These features are congruent with the results of *Lu et al.*

[2010], who observed the production of a TGF during the upward development of an IC leader reflected by a slowly building current moment punctuated by impulsive discharges. The presence of multiple VLF impulses both during and prior to the slow pulse can lead to ambiguity in the interpretation of the temporal relationship between lightning and TGF. It is feasible that the observations of $\Delta t \sim 4$–8 ms might be caused by matching of TGFs to precursor sferics [*Lu et al.*, 2011].

4.5. Distance and Spectrum

[86] The γ-ray spectra observed at satellite altitude have been used to infer various characteristics of TGFs [*Østgaard et al.*, 2008; *Grefenstette et al.*, 2008; *Hazelton et al.*, 2009], but these studies have been encumbered by uncertainty in the relative location of the TGF sources. This analysis finds that TGFs are observed at angles out to $\alpha = 52°$, with the highest density occurring at $\alpha = 17°$.

[87] The average RHESSI TGF has only 25 photons, which is not far above the detection threshold. Fainter events are not identified because they are submerged in the background. The spectrum of an individual RHESSI TGF is thus poorly described by the paltry number of photons collected. Spectra from a number of events have thus been averaged to achieve reasonable statistics [e.g., *Dwyer and Smith*, 2005]. However, in the process, inherently different spectra originating from events at different distances have been combined, thereby discarding much information. *Hazelton et al.* [2009] partially overcame this difficulty by partitioning TGFs according to whether or not they were associated with thunderstorms closer than 300 km from the sub-satellite point, and observed softer spectra for TGFs linked to more distant storms. With the collection of matched events presented here it is now possible to group the TGFs into sets originating within a selection of distance intervals and form averages which are both statistically reliable and also representative of the effects of propagation. Such an analysis has been presented by *Gjesteland et al.* [2011].

5. Conclusion

[88] Using a simple coincidence algorithm, 93 of the 972 TGFs detected by RHESSI between 4 March 2002 and 6 September 2010 were matched to individual lightning discharges identified by WWLLN. On average the TGFs were found to precede the associated lightning events, with a mean delay of −0.77 ms. This observation is consistent with the idea that TGFs are produced during the initial formative stages of a lightning discharge. The TGFs which were uniquely matched to a causative lightning discharge were found to have intensities which were generally smaller than those for the entire sample of TGFs. This indicates that the intense lightning which is preferentially detected by WWLLN might be linked to weaker TGFs. Finally, the average number of photons per matched TGF appears to be independent of the distance between the lightning and the satellite, which supports the hypothesis of a power law distribution for TGF intensity.

References

Abadie, A. (2002), Bootstrap tests for distributional treatment effects in instrumental variable models, *J. Am. Stat. Assoc.*, 97(457), 284–292.

Abarca, S. F., K. L. Corbosiero, and T. J. Galarneau Jr. (2010), An evaluation of the Worldwide Lightning Location Network (WWLLN) using the National Lightning Detection Network (NLDN) as ground truth, *J. Geophys. Res.*, 115, D18206, doi:10.1029/2009JD013411.

Briggs, M. S., et al. (2010), First results on terrestrial gamma ray flashes from the Fermi Gamma-ray Burst Monitor, *J. Geophys. Res.*, 115, A07323, doi:10.1029/2009JA015242.

Briggs, M. S., et al. (2011), Electron-positron beams from terrestrial lightning observed with Fermi GBM, *Geophys. Res. Lett.*, 38, L02808, doi:10.1029/2010GL046259.

Carlson, B. E., N. G. Lehtinen, and U. S. Inan (2007), Constraints on terrestrial gamma ray flash production from satellite observation, *Geophys. Res. Lett.*, 34, L08809, doi:10.1029/2006GL029229.

Carlson, B. E., N. G. Lehtinen, and U. S. Inan (2008), Runaway relativistic electron avalanche seeding in the Earth's atmosphere, *J. Geophys. Res.*, 113, A10307, doi:10.1029/2008JA013210.

Carlson, B. E., N. G. Lehtinen, and U. S. Inan (2009), Terrestrial gamma ray flash production by lightning current pulses, *J. Geophys. Res.*, 114, A00E08, doi:10.1029/2009JA014531.

Carlson, B. E., N. G. Lehtinen, and U. S. Inan (2010), Terrestrial gamma ray flash production by active lightning leader channels, *J. Geophys. Res.*, 115, A10324, doi:10.1029/2010JA015647.

Christian, H. J., R. J. Blakeslee, D. J. Boccippio, W. L. Boeck, D. E. Buechler, K. T. Driscoll, S. J. Goodman, J. M. Hall, W. J. Koshak, D. M. Mach, and M. F. Stewart (2003), Global frequency and distribution of lightning as observed from space by the Optical Transient Detector, *J. Geophys. Res.*, 108(D1), 4005, doi:10.1029/2002JD002347.

Chronis, T. G., and E. N. Anagnostou (2003), Error analysis for a long-range lightning monitoring network of ground-based receivers in Europe, *J. Geophys. Res.*, 108(D24), 4779, doi:10.1029/2003JD003776.

Clauset, A., C. R. Shalizi, and M. E. J. Newman (2009), Power-law distributions in empirical data, *SIAM Rev.*, 51(4), 661–703, doi:10.1137/070710111.

Cohen, M. B., U. S. Inan, and G. J. Fishman (2006), Terrestrial gamma ray flashes observed aboard the Compton Gamma Ray Observatory/Burst and Transient Source Experiment and ELF/VLF radio atmospherics, *J. Geophys. Res.*, 111, D24109, doi:10.1029/2005JD006987.

Cohen, M. B., U. S. Inan, R. K. Said, and T. Gjesteland (2010), Geolocation of terrestrial gamma-ray flash source lightning, *Geophys. Res. Lett.*, 37, L02801, doi:10.1029/2009GL041753.

Connaughton, V., et al. (2010a), Associations between Fermi Gamma-ray Burst Monitor terrestrial gamma ray flashes and sferics from the World Wide Lightning Location Network, *J. Geophys. Res.*, 115, A12307, doi:10.1029/2010JA015681.

Connaughton, V., M. S. Briggs, S. Xiong, M. L. Hutchins, R. H. Holzworth, G. J. Fishman, and D. M. Smith (2010b), What can geolocated sferics tell us about terrestrial gamma-ray flashes?, Abstract AE11A-0331 presented at 2010 Fall Meeting, AGU, San Francisco, Calif., 13–17 Dec.

Cummer, S. A., Y. Zhai, W. Hu, D. M. Smith, L. I. Lopez, and M. A. Stanley (2005), Measurements and implications of the relationship between lightning and terrestrial gamma ray flashes, *Geophys. Res. Lett.*, 32, L08811, doi:10.1029/2005GL022778.

Dowden, R. L., J. B. Brundell, and C. J. Rodger (2002), VLF lightning location by time of group arrival (TOGA) at multiple sites, *J. Atmos. Sol. Terr. Phys.*, 64(7), 817–830, doi:10.1016/S1364-6826(02)00085-8.

Dowden, R. L., et al. (2008), World-wide lightning location using VLF propagation in the Earth-ionosphere waveguide, *IEEE Antennas Propag. Mag.*, 50(5), 40–60, doi:10.1109/MAP.2008.4674710.

Dwyer, J. R. (2003), A fundamental limit on electric fields in air, *Geophys. Res. Lett.*, 30(20), 2055, doi:10.1029/2003GL017781.

Dwyer, J. R. (2007), Relativistic breakdown in planetary atmospheres, *Phys. Plasmas*, 14, 042901, doi:10.1063/1.2709652.

Dwyer, J. R. (2008), Source mechanisms of terrestrial gamma-ray flashes, *J. Geophys. Res.*, 113, D10103, doi:10.1029/2007JD009248.

Dwyer, J. R., and D. M. Smith (2005), A comparison between Monte Carlo simulations of runaway breakdown and terrestrial gamma-ray flash observations, *Geophys. Res. Lett.*, 32, L22804, doi:10.1029/2005GL023848.

Dwyer, J. R., et al. (2005), X-ray bursts associated with leader steps in cloud-to-ground lightning, *Geophys. Res. Lett.*, 32, L01803, doi:10.1029/2004GL021782.

Dwyer, J. R., B. W. Grefenstette, and D. M. Smith (2008), High-energy electron beams launched into space by thunderstorms, *Geophys. Res. Lett.*, 35, L02815, doi:10.1029/2007GL032430.

Fishman, G. J., et al. (1994), Discovery of intense gamma-ray flashes of atmospheric origin, *Science*, 264(5163), 1313–1316, doi:10.1126/science.264.5163.1313.

Gjesteland, T., N. Østgaard, P. H. Connell, J. Stadsnes, and G. J. Fishman (2010), Effects of dead time losses on terrestrial gamma ray flash measurements with the Burst and Transient Source Experiment, *J. Geophys. Res.*, 115, A00E21, doi:10.1029/2009JA014578.

Gjesteland, T., N. Østgaard, A. B. Collier, B. E. Carlson, M. B. Cohen, and N. G. Lehtinen (2011), Confining the angular distribution of terrestrial gamma-ray flash emission, *J. Geophys. Res.*, doi:10.1029/2011JA016716, in press.

Grefenstette, B. W., D. M. Smith, J. R. Dwyer, and G. J. Fishman (2008), Time evolution of terrestrial gamma ray flashes, *Geophys. Res. Lett.*, 35, L06802, doi:10.1029/2007GL032922.

Grefenstette, B. W., D. M. Smith, B. J. Hazelton, and L. I. Lopez (2009), First RHESSI terrestrial gamma ray flash catalog, *J. Geophys. Res.*, 114, A02314, doi:10.1029/2008JA013721.

Gurevich, A. V., and G. M. Milikh (1999), Generation of X-rays due to multiple runaway breakdown inside thunderclouds, *Phys. Lett. A*, 262(6), 457–463, doi:10.1016/S0375-9601(99)00695-7.

Gurevich, A. V., G. M. Milikh, and R. A. Roussel-Dupré (1992), Runaway electron mechanism of air breakdown and preconditioning during a thunderstorm, *Phys. Lett. A*, 165(5–6), 463–468, doi:10.1016/0375-9601(92)90348-P.

Hazelton, B. J., B. W. Grefenstette, D. M. Smith, J. R. Dwyer, X. -M. Shao, S. A. Cummer, T. G. Chronis, E. H. Lay, and R. H. Holzworth (2009), Spectral dependence of terrestrial gamma-ray flashes on source distance, *Geophys. Res. Lett.*, 36, L01108, doi:10.1029/2008GL035906.

Howard, J., M. A. Uman, J. R. Dwyer, D. Hill, C. Biagi, Z. Saleh, J. Jerauld, and H. K. Rassoul (2008), Co-location of lightning leader x-ray and electric field change sources, *Geophys. Res. Lett.*, 35, L13817, doi:10.1029/2008GL034134.

Inan, U. S., and N. G. Lehtinen (2005), Production of terrestrial gamma-ray flashes by an electromagnetic pulse from a lightning return stroke, *Geophys. Res. Lett.*, 32, L19818, doi:10.1029/2005GL023702.

Inan, U. S., S. C. Reising, G. J. Fishman, and J. M. Horack (1996), On the association of terrestrial gamma ray bursts with lightning and implications for sprites, *Geophys. Res. Lett.*, 23(9), 1017–1020, doi:10.1029/96GL00746.

Inan, U. S., M. B. Cohen, R. K. Said, D. M. Smith, and L. I. Lopez (2006), Terrestrial gamma ray flashes and lightning discharges, *Geophys. Res. Lett.*, 33, L18802, doi:10.1029/2006GL027085.

Jacobson, A. R., R. H. Holzworth, J. Harlin, R. L. Dowden, and E. H. Lay (2006), Performance assessment of the World Wide Lightning Location Network (WWLLN), using the Los Alamos Sferic Array (LASA) as ground truth, *J. Atmos. Oceanic Technol.*, 23(8), 1082–1092, doi:10.1175/JTECH1902.1.

Lay, E. H. (2008), Investigating lightning-to-ionosphere energy coupling based on VLF lightning propagation characterization, Ph.D. dissertation, Univ. of Wash., Seattle.

Lay, E. H., R. H. Holzworth, C. J. Rodger, J. N. Thomas, O. Pinto Jr., and R. L. Dowden (2004), WWLL global lightning detection system: Regional validation study in Brazil, *Geophys. Res. Lett.*, 31, L03102, doi:10.1029/2003GL018882.

Lay, E. H., A. R. Jacobson, R. H. Holzworth, C. J. Rodger, and R. L. Dowden (2007), Local time variation in land/ocean lightning flash density as measured by the World Wide Lightning Location Network, *J. Geophys. Res.*, 112, D13111, doi:10.1029/2006JD007944.

Lehtinen, N. G., M. Walt, U. S. Inan, T. F. Bell, and V. P. Pasko (1996), γ-ray emission produced by a relativistic beam of runaway electrons accelerated by quasi-electrostatic thundercloud fields, *Geophys. Res. Lett.*, 23(19), 2645–2648, doi:10.1029/96GL02573.

Lehtinen, N. G., T. F. Bell, and U. S. Inan (1999), Monte Carlo simulation of runaway MeV electron breakdown with application to red sprites and terrestrial gamma ray flashes, *J. Geophys. Res.*, 104(A11), 24,699–24,712, doi:10.1029/1999JA900335.

Lehtinen, N. G., U. S. Inan, and T. F. Bell (2001), Effects of thunderstorm-driven runaway electrons in the conjugate hemisphere: Purple sprites,

ionization enhancements, and gamma rays, *J. Geophys. Res.*, *106*(A12), 28,841–28,856, doi:10.1029/2000JA000160.

Li, J., S. A. Cummer, W. A. Lyons, and T. E. Nelson (2008), Coordinated analysis of delayed sprites with high-speed images and remote electromagnetic fields, *J. Geophys. Res.*, *113*, D20206, doi:10.1029/2008JD010008.

Lu, G., R. J. Blakeslee, J. Li, D. M. Smith, X. -M. Shao, E. W. McCaul, D. E. Buechler, H. J. Christian, J. M. Hall, and S. A. Cummer (2010), Lightning mapping observation of a terrestrial gamma-ray flash, *Geophys. Res. Lett.*, *37*, L11806, doi:10.1029/2010GL043494.

Lu, G., S. A. Cummer, J. Li, F. Han, D. M. Smith, and B. W. Grefenstette (2011), Characteristics of broadband lightning emissions associated with terrestrial gamma ray flashes, *J. Geophys. Res.*, *116*, A03316, doi:10.1029/2010JA016141.

Lyons, W. A. (1996), Sprite observations above the U.S. high plains in relation to their parent thunderstorm systems, *J. Geophys. Res.*, *101*(D23), 29,641–29,652, doi:10.1029/96JD01866.

Mackerras, D., M. Darveniza, R. E. Orville, E. R. Williams, and S. J. Goodman (1998), Global lightning: Total, cloud, and ground flash estimates, *J. Geophys. Res.*, *103*(D16), 19,791–19,809.

Marisaldi, M., et al. (2010), Detection of terrestrial gamma ray flashes up to 40 MeV by the AGILE satellite, *J. Geophys. Res.*, *115*, A00E13, doi:10.1029/2009JA014502.

McCarthy, M. P., and G. K. Parks (1985), Further observations of X-rays inside thunderstorms, *Geophys. Res. Lett.*, *12*(6), 393–396, doi:10.1029/GL012i006p00393.

Milikh, G., and J. A. Valdivia (1999), Model of gamma ray flashes due to fractal lightning, *Geophys. Res. Lett.*, *26*(4), 525–528, doi:10.1029/1999GL900001.

Milikh, G. M., and R. Roussel-Dupré (2010), Runaway breakdown and electrical discharges in thunderstorms, *J. Geophys. Res.*, *115*, A00E60, doi:10.1029/2009JA014818.

Moore, C. B., K. B. Eack, G. D. Aulich, and W. Rison (2001), Energetic radiation associated with lightning stepped-leaders, *Geophys. Res. Lett.*, *28*(11), 2141–2144, doi:10.1029/2001GL013140.

Moss, G. D., V. P. Pasko, N. Liu, and G. Veronis (2006), Monte Carlo model for analysis of thermal runaway electrons in streamer tips in transient luminous events and streamer zones of lightning leaders, *J. Geophys. Res.*, *111*, A02307, doi:10.1029/2005JA011350.

Mushtak, V. C., E. R. Williams, and D. J. Boccippio (2005), Latitudinal variations of cloud base height and lightning parameters in the tropics, *Atmos. Res.*, *76*(1–4), 222–230, doi:10.1016/j.atmosres.2004.11.010.

Nemiroff, R. J., J. T. Bonnell, and J. P. Norris (1997), Temporal and spectral characteristics of terrestrial gamma flashes, *J. Geophys. Res.*, *102*(A5), 9659–9665, doi:10.1029/96JA03107.

Nguyen, C. V., A. P. J. van Deursen, and U. Ebert (2008), Multiple X-ray bursts from long discharges in air, *J. Phys. D Appl. Phys.*, *41*, 234012, doi:10.1088/0022-3727/41/23/234012.

Østgaard, N., T. Gjesteland, J. Stadsnes, P. H. Connell, and B. E. Carlson (2008), Production altitude and time delays of the terrestrial gamma flashes: Revisiting the Burst and Transient Source Experiment spectra, *J. Geophys. Res.*, *113*, A02307, doi:10.1029/2007JA012618.

Orville, R. E., and G. R. Huffines (2001), Cloud-to-ground lightning in the United States: NLDN results in the first decade, 1989–98, *Mon. Weather Rev.*, *129*, 1179–1193, doi:10.1175/1520-0493(2001)129<1179:CTGLIT>2.0.CO;2.

Reeves, M. C., R. H. Holzworth, A. R. Jacobson, M. P. McCarthy, M. L. Hutchins, and R. F. Pfaff (2010), Global optical lightning intensity near the equator from the C/NOFS satellite, Abstract AE21B-0277 presented at 2010 Fall Meeting, AGU, San Francisco, Calif., 13–17 Dec.

Rodger, C. J., J. B. Brundell, and R. L. Dowden (2005), Location accuracy of VLF World-Wide Lightning Location (WWLL) network: Post-algorithm upgrade, *Annales Geophysicae*, *23*(2), 277–290.

Rodger, C. J., S. Werner, J. B. Brundell, E. H. Lay, N. R. Thomson, R. H. Holzworth, and R. L. Dowden (2006), Detection efficiency of the VLF World-Wide Lightning Location Network (WWLLN): Initial case study, *Ann. Geophys.*, *24*, 3197–3214.

Rodger, C. J., J. B. Brundell, and R. H. Holzworth (2009a), Improvements in the WWLLN: Bigger detection efficiencies through more stations and smarter algorithms, paper presented at 11th IAGA Scientific Assembly, Sopron, Hungary.

Rodger, C. J., J. B. Brundell, R. H. Holzworth, and E. H. Lay (2009b), Growing detection efficiency of the World Wide Lightning Location Network, in *Coupling of Thunderstorms and Lightning Discharges to Near-Earth Space: Proceedings of the Workshop, Corte, France, 23–27 June 2008*, vol. 1118, edited by N. B. Crosby, T.-Y. Huang, and M. J. Rycroft, pp. 15–20, Am. Inst. of Phys., Melville, N. Y., doi:10.1063/1.3137706.

Roussel-Dupré, R. A., E. Symbalisty, Y. Taranenko, and V. Yukhimuk (1998), Simulations of high-altitude discharges initiated by runaway breakdown, *J. Atmos. Sol. Terr. Phys.*, *60*(7–9), 917–940, doi:10.1016/S1364-6826(98)00028-5.

Sentman, D. D., and E. M. Wescott (1995), Red sprites and blue jets: Thunderstorm-excited optical emissions in the stratosphere, mesosphere and ionosphere, *Phys. Plasmas*, *2*(6), 2514–2522, doi:10.1063/1.871213.

Shao, X.-M., T. Hamlin, and D. M. Smith (2010), A closer examination of terrestrial gamma-ray flash-related lightning processes, *J. Geophys. Res.*, *115*, A00E30, doi:10.1029/2009JA014835.

Smith, D. A., K. B. Eack, J. Harlin, M. J. Heavner, A. R. Jacobson, R. S. Massey, X. M. Shao, and K. C. Wiens (2002a), The Los Alamos Sferic Array: A research tool for lightning investigations, *J. Geophys. Res.*, *107*(D13), 4183, doi:10.1029/2001JD000502.

Smith, D. M., et al. (2002b), The RHESSI spectrometer, *Sol. Phys.*, *210*(1), 33–60, doi:10.1023/A:1022400716414.

Smith, D. M., L. I. Lopez, R. P. Lin, and C. P. Barrington-Leigh (2005), Terrestrial gamma-ray flashes observed up to 20 MeV, *Science*, *307*(5712), 1085–1088, doi:10.1126/science.1107466.

Smith, D. M., et al. (2006), The anomalous terrestrial gamma-ray flash of 17 January 2004, *Eos Trans. AGU*, Fall Meet. Suppl., *87*(52), Abstract AE31A-1040.

Smith, D. M., B. J. Hazelton, B. W. Grefenstette, J. R. Dwyer, R. H. Holzworth, and E. H. Lay (2010), Terrestrial gamma ray flashes correlated to storm phase and tropopause height, *J. Geophys. Res.*, *115*, A00E49, doi:10.1029/2009JA014853.

Smith, D. M., et al. (2011), The rarity of terrestrial gamma-ray flashes, *Geophys. Res. Lett.*, *38*, L08807, doi:10.1029/2011GL046875.

Splitt, M. E., S. M. Lazarus, D. Barnes, J. R. Dwyer, H. K. Rassoul, D. M. Smith, B. J. Hazelton, and B. W. Grefenstette (2010), Thunderstorm characteristics associated with RHESSI identified terrestrial gamma ray flashes, *J. Geophys. Res.*, *115*, A00E38, doi:10.1029/2009JA014622.

Stanley, M. A., X.-M. Shao, D. M. Smith, L. I. Lopez, M. B. Pongratz, J. D. Harlin, M. Stock, and A. Regan (2006), A link between terrestrial gamma-ray flashes and intracloud lightning discharges, *Geophys. Res. Lett.*, *33*, L06803, doi:10.1029/2005GL025537.

Watkins, N. W., M. A. Clilverd, A. J. Smith, C. J. Rodger, N. A. Bharmal, and K. H. Yearby (2001), Lightning atmospherics count rates observed at Halley, Antarctica, *J. Atmos. Sol. Terr. Phys.*, *63*(10), 993–1003.

Williams, E. R., and G. Sátori (2004), Lightning, thermodynamic and hydrological comparison of the two tropical continental chimneys, *J. Atmos. Sol. Terr. Phys.*, *66*(13–14), 1213–1231, doi:10.1016/j.jastp.2004.05.015.

Williams, E. R., M. E. Weber, and R. E. Orville (1989), The relationship between lightning type and convective state of thunderclouds, *J. Geophys. Res.*, *94*(D11), 13,213–13,220, doi:10.1029/JD094iD11p13213.

Williams, E. R., et al. (2006), Lightning flashes conducive to the production and escape of gamma radiation to space, *J. Geophys. Res.*, *111*, D16209, doi:10.1029/2005JD006447.

Wilson, C. T. R. (1925), The acceleration of β-particles in strong electric fields such as those of thunderclouds, *Math. Proc. Cambridge Philos. Soc.*, *22*(4), 534–538, doi:10.1017/S0305004100003236.

A. B. Collier, SANSA Space Science, PO Box 32, Hermanus, 7200 South Africa. (collierab@gmail.com)

T. Gjesteland and N. Østgaard, Department of Physics and Technology, University of Bergen, Postboks 7803, Bergen N-5020, Norway. (thomas.gjesteland@uib.no; nikolai.ostgaard@ift.uib.no)